Single-shot x-ray absorption at soft x-ray free-electron-laser facilities: what we may learn

A. Di Cicco, R. Gunnella, K. Hatada*, A. Trapananti

Università di Camerino, Italy
**Toyama University, Japan*

SILS 2019 Meeting
Camerino 9-11 September

TIMEX collaboration 2007-2013 - (ELETTRA resp.: C. Masciovecchio): F. Bencivenga, R. Cucini, F. D'Amico, S. Di Fonzo, A. Filipponi, E. Giangrisostomi, R. Gunnella, K. Hatada, E. Principi, L. Properzi, A. Trapananti

Ultra-short x-ray pulses

Short pulses from synchrotron radiation sources (slicing) – order of 100 MHz repetition rates

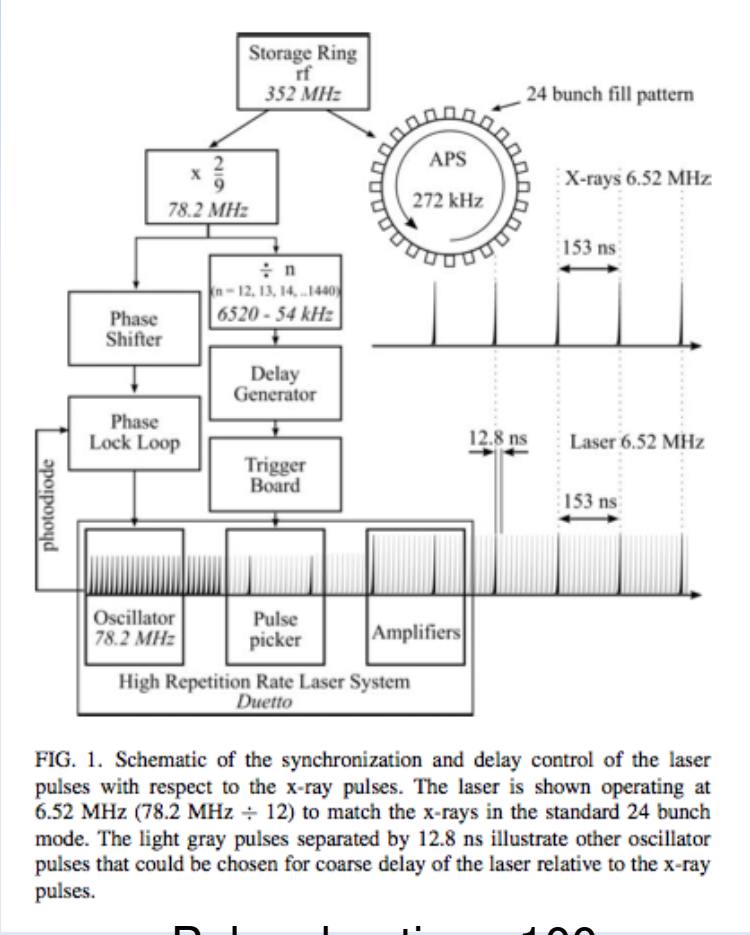

FIG. 1. Schematic of the synchronization and delay control of the laser pulses with respect to the x-ray pulses. The laser is shown operating at 6.52 MHz (78.2 MHz ÷ 12) to match the x-rays in the standard 24 bunch mode. The light gray pulses separated by 12.8 ns illustrate other oscillator pulses that could be chosen for coarse delay of the laser relative to the x-ray pulses.

Pulse duration ~100 ps

Free Electron Laser

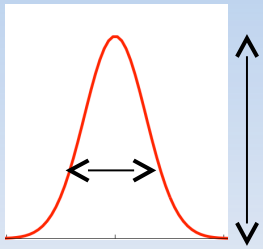

Short pulse

High intensity

currently 10-100 Hz repetition rate

XFEL 27 kHz

Ex. SACLA below 10fs with 10^{18}W/cm^2

Faster than electron-phonon interaction, comparable to the lifetime of core-hole

Non-linear optical effects on ultra short time resolved spectroscopies

Average photon flux is similar

Typical peak brightness

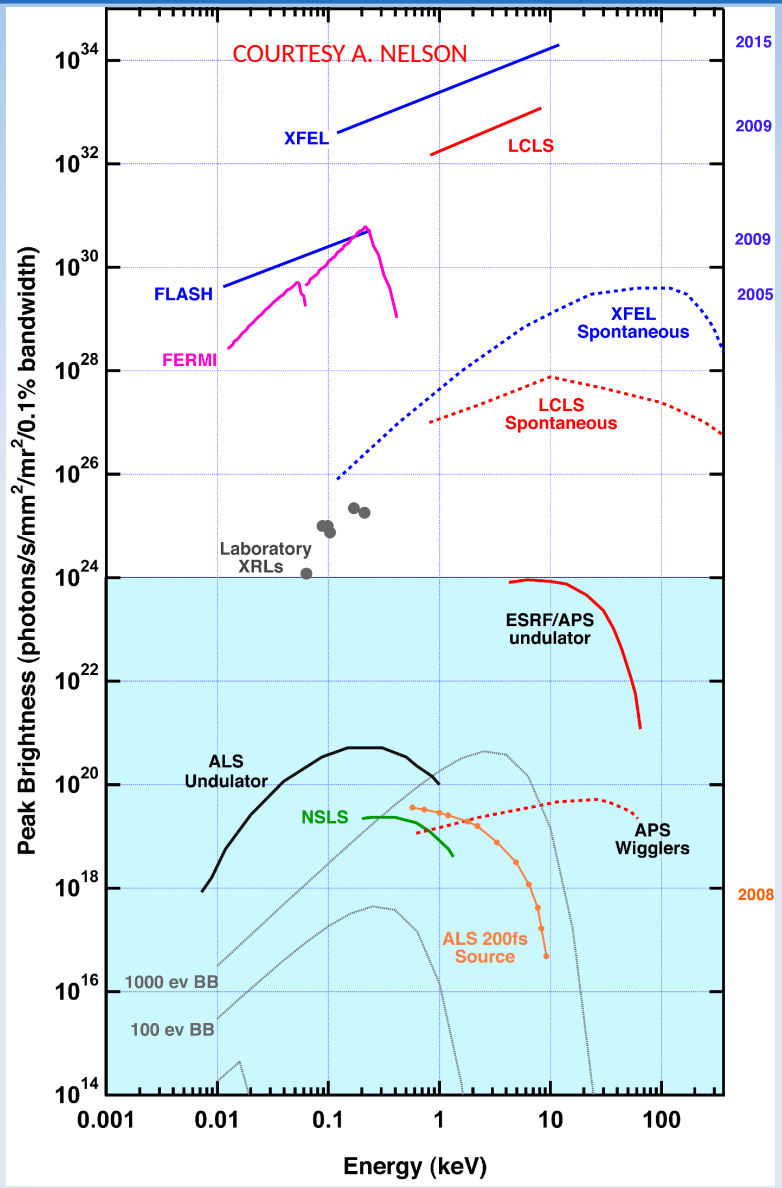

- Peak brightness of FELs are several order of magnitude highers of those of synchrotrons.
- Slow repetition rates for most FELs (10-200 Hz as compared to ~100 MHz in storage rings) limits the average flux.
- Single-shot experiments.

Parameter	FEL - 1	FEL - 2	Units
Wavelength	100 - 20	20 - 3	nm
Photon Energy	12 - 62	62 - 413	eV
Pulse Length	30 - 100	< 100	fs
Bandwidth	~ 20 - 40	~ 20 - 40	meV
Polarization	variable	variable	-
Repetition Rate	10 - 50	10 - 50	Hz
Peak Power	1 ÷ 5	~ 1	GW
Photons per Pulse	$2 \cdot 10^{14}$ @ 100 nm	$1 \cdot 10^{13}$ @ 10 nm	-
Power Fluctuation	~ 25%	> 50%	-
Central Wavelength Fluctuation	within bandwidth	within bandwidth	-
Output Transverse Position Fluctuation	50	50	μm
Pointing Fluctuation	< 5	< 5	μrad
Output Spot Size (intensity, FWHM@waist)	290	140	μm
Divergence (intensity, RMS)	50 @ 40 nm	15 @ 10 nm	μrad

- Fermi@Elettra parameters

Courtesy of F. Parmigiani, W. Fawley & E. Allaria

TIMEX project (http://gnxas.unicam.it/TIMEX)

- **Our previous experience:**
- TIMEX end-station proposal (2006): TIme-resolved studies of Matter under EXtreme and metastable conditions

See report on Notiziario Neutroni e Luce di Sincrotrone 26 Volume 18 n. 2 (July 2013)

- EIS beamline including TIMEX approved (UniCam-ELETTRA agreement 2007-2012)

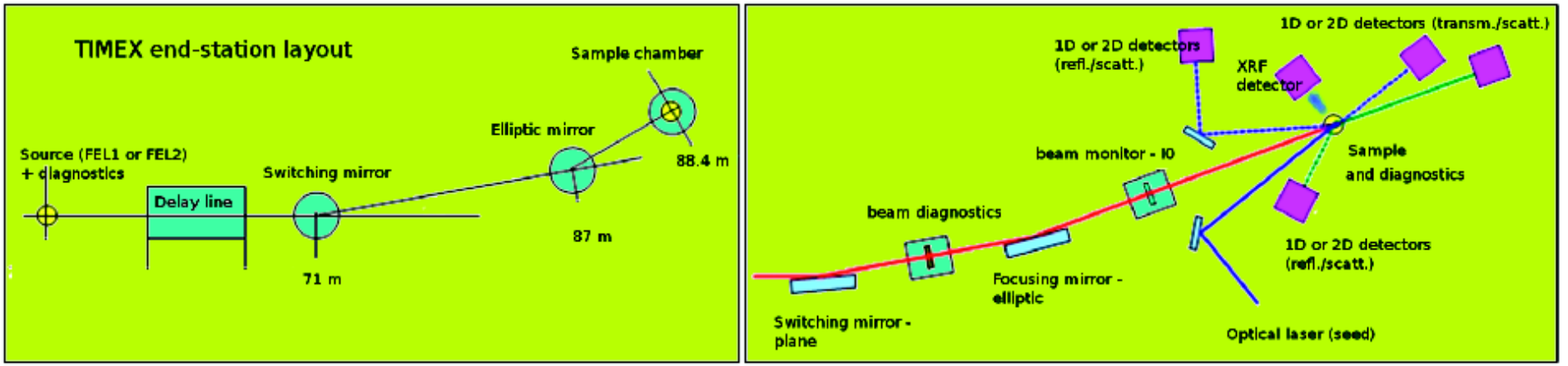

Figure 1

Sketch of the TIMEX end-station under commissioning at the FERMI@Elettra FEL facility. The left side shows the main components of the beamline, including the delay line and the elliptic mirror that should be installed after a performance test, within a few months. In the right side, we show some details of the focusing and aligning devices and the detectors used for reflection, transmission, scattering and x-ray emission (XRF) measurements using both FEL and optical laser pulses. The pump-probe scheme should be tested within a few months.

Commissioning the TIMEX end-station

- Design of the end-station and place of orders completed in June 2010. Vacuum chambers delivered in late October 2010. Pilot experiments (2007-2010) completed. Assembling and test of the main components of the TIMEX end-station in the main Fermi hall started in December 2010.
- The TIMEX optics (C. Svetina, D. Cocco) did not match specifications (SESO manifacturing) and were delivered with 3 years delay. All tests and first runs (for a total of ~3 weeks of beamtime) since March 2011 using a simplified optics.
- Beamline open to users since the first call for proposals. Optics delivered and installed in late 2013, pump-probe (laser-seed + FEL) installed and tested (late 2013).
- Personnel/contacts: C. Masciovecchio group (main responsible E. Principi)

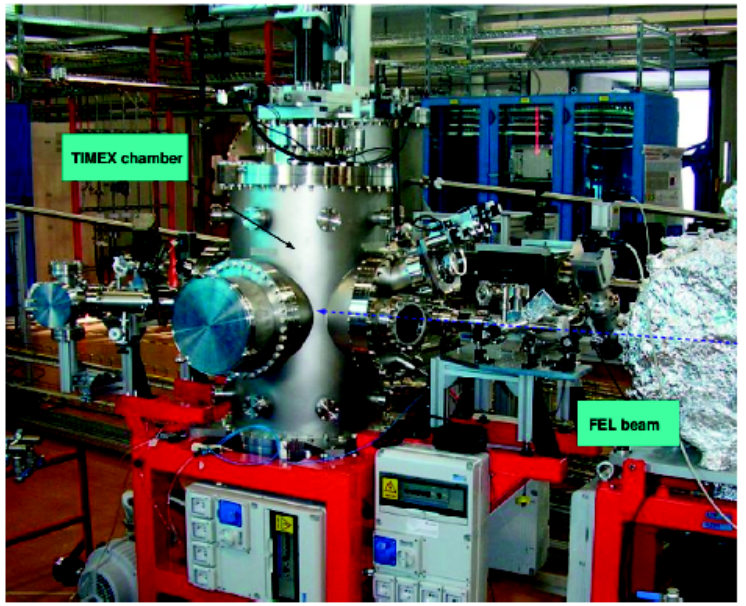

Figure 2

Picture of the TIMEX chamber installed and aligned at the exit of the FEL1 source in 2012. The FEL beam (blue dashed line, guide for the eye) has been aligned up to the main TIMEX chamber, where the sample position can be controlled with a 5-axis motorized manipulator while the transmitted and reflected pulses were measured by the photodiodes and thermopiles.

Assembling the TIMEX UHV chamber in the main -empty- Fermi hall (17 nov 2010)

Bulk heating 20-200 eV photons

- Quasi-isotherm bulk heating can be obtained by using FEL1 pulses on several films (Al, Si, Ge, and more)
- Electron temperatures are estimated to be in the range 1-10 eV (WDM regime)
- Large-sized self-standing films are robust (0.1-0.3 microns thickness) and can be used for shot-to-shot experiments at the FEL repetition rate
- FEL2 useful for bulk heating of some important material (C for example)
- → Soft x-ray FELs are really useful for efficient bulk heating!

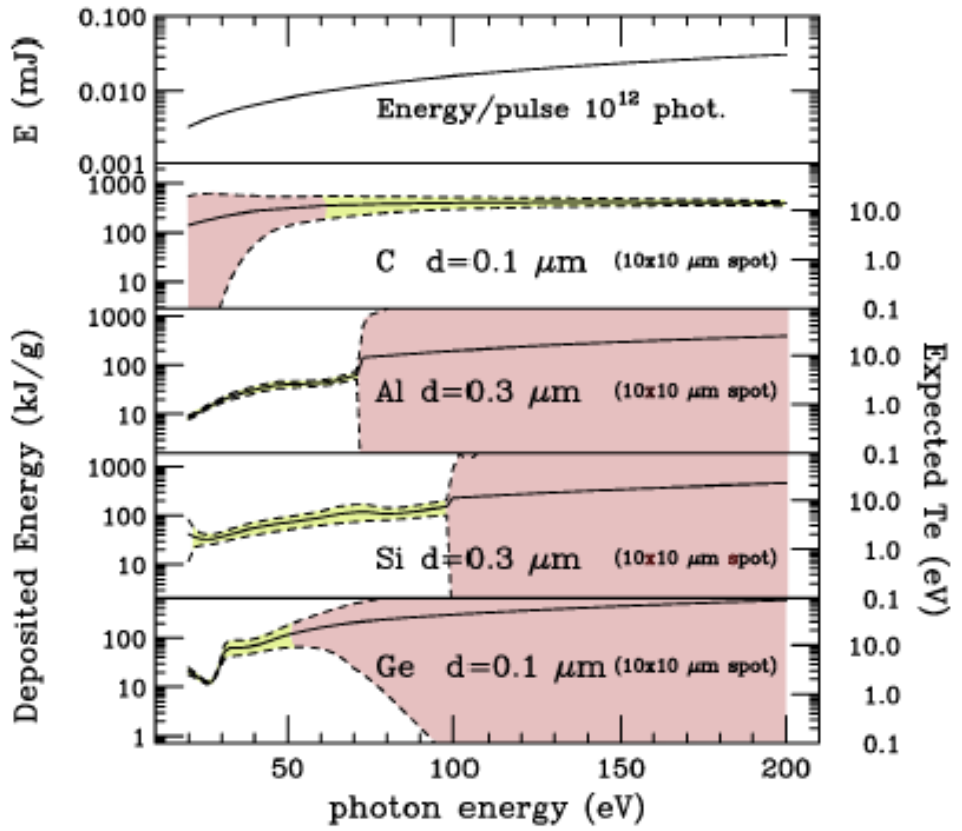

Figure 4. In the lower four panels we report the deposited energy (kJ per gram of substance) in different thin film materials as a function of the photon energy for a pulse containing 10^{12} photons (spot 10x10 μm). The deposited energy (solid curves) has been calculated accounting for possible saturation effects and show different trends according to the particular foil under consideration. The dashed curves represent the limits for the spread of deposited energy inside the films, so uniform bulk heating is obtained when the dashed curves define a narrow region (light green, color on-line). On the other hand, when most of the energy is deposited near the surface of the thin film, an extremely inhomogeneous heating is obtained (pink regions, color on-line). The expected electron temperature T_e is also shown on the right axis, showing that average temperatures in the 1-10 eV range are easily reached depending on the energy and thin foil material. The upper panel reports the pulse energy (mJ) as a function of the photon energy (eV) obviously changing of 1 order of magnitude from 20 to 200 eV. The FEL1 source (12-62 eV) turns out to be extremely efficient for obtaining uniform bulk heating of various materials (for example Al, Si, Ge shown in the picture).

Ultrafast excitation of the Si(100) surface: pictorial view

PHYSICAL REVIEW B 73, 134108 (2006)

Thermodynamic pathways to melting, ablation, and solidification in absorbing solids under pulsed laser irradiation

Patrick Lorazo,[1,2] Laurent J. Lewis,[2,*] and Michel Meunier[1,†]

·A combined MC and MD calculation on a (100) slab of 142560 atoms was used to calculate the thermodynamic pathway after excitation (500 fs pulse). Rapid non-thermal disordering and nearly isochoric heating (B) of the metallic liquid is followed by cooling in the liquid-vapor regime.

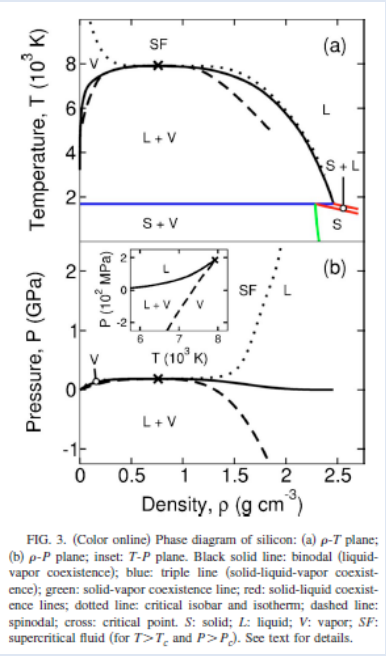

FIG. 3. (Color online) Phase diagram of silicon: (a) ρ-T plane; (b) ρ-P plane; inset: T-P plane. Black solid line: binodal (liquid-vapor coexistence); blue: triple line (solid-liquid-vapor coexistence); green: solid-vapor coexistence line; red: solid-liquid coexistence lines; dotted line: critical isobar and isotherm; dashed line: spinodal; cross: critical point. S: solid; L: liquid; V: vapor; SF: supercritical fluid (for $T>T_c$ and $P>P_c$). See text for details.

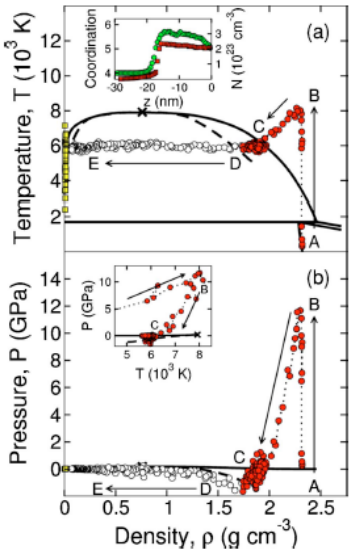

FIG. 5. (Color online) Time evolution of the system in the (a) ρ-T and (b) ρ-P planes for a 500 fs pulse at a fluence $F=F_{th}^{fs}=0.225$ J cm^{-2}; the trajectory is for a region of the target initially at a depth of 4 nm below the surface. White circles and dotted line: macroscopic branch; red circles: dense branch; yellow squares: gas branch. Arrows indicate the flow of time. Capital letters refer to locations in the phase diagram (see text). Insets: (a) coordination (green circles) and electron density N (red squares) as a function of distance from the surface z at $t=1$ ps (note the change in properties across the solid-liquid interface at $z\approx-18$ nm); (b) view of the trajectory in the T-P plane.

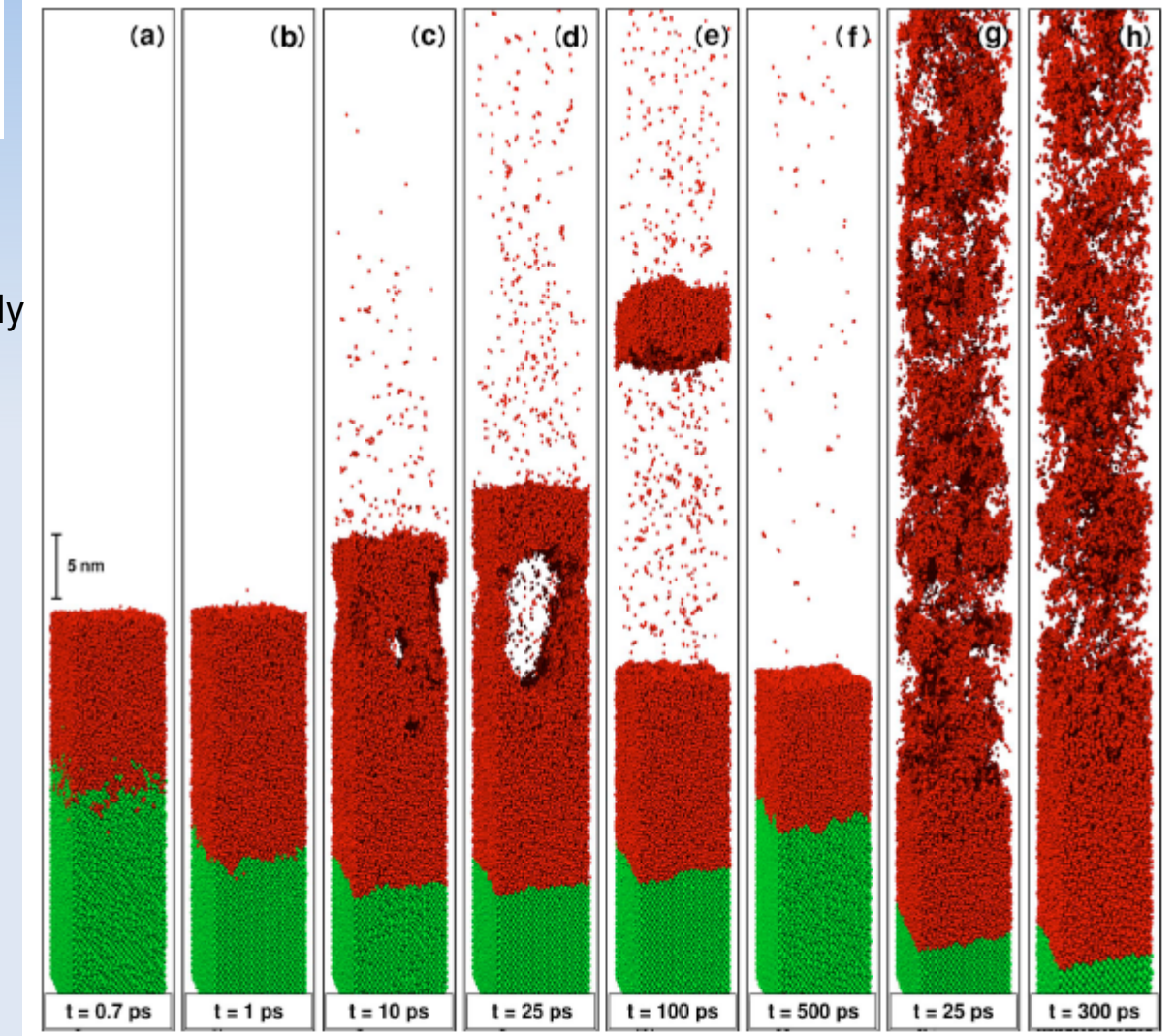

FIG. 4. (Color online) Snapshots revealing the structural changes induced in a Si(100) substrate by 500 fs and 100 ps pulses at 266 nm: (a)–(f) 500 fs pulse at a fluence $F=F_{th}^{fs}=0.225$ J cm^{-2}; (g) 500 fs pulse at a fluence $F=2.2F_{th}^{fs}=0.50$ J cm^{-2}; (h) 100 ps pulse at a fluence $F=1.1F_{th}^{ns}=0.45$ J cm^{-2}; F_{th}^{fs} and F_{th}^{ns} are the ablation thresholds under femtosecond and picosecond irradiation, respectively. Green: (semiconducting) crystalline silicon; red: (metallic) liquid silicon. Each pulse begins at $t=0$.

FEL radiation is able to create and/or probe WDM in an extended P-T range

- *WDM occurs at high temperatures/ high pressure regimes: core of large planets and experiments relevant to inertial fusion, in the transition from solids to plasma*
- *Lack of knowledge in the Equation of State (EOS) even of simple systems near WDM regime (data largely based on single-shot shock-wave techniques)*
- *During a typical WDM creation,* systems usually start solid and end as a plasma. FEL radiation can heat bulk matter rapidly and uniformly to create isochores (constant density- red) and isoentropies on release (constant entropy -blue).*

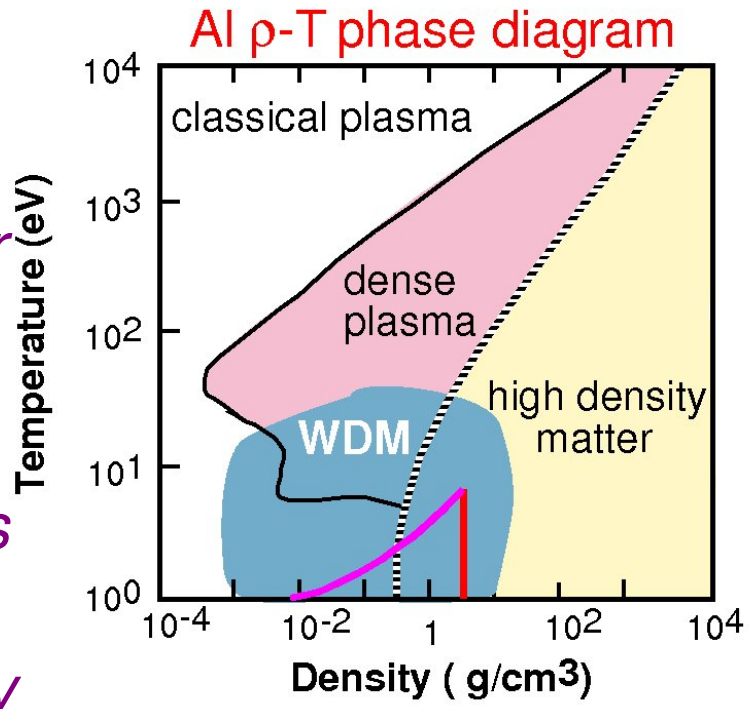

** see for example B. Nagler et al., Nat. Phys. 5, 693 (2009).*

TIMEX initial layout details

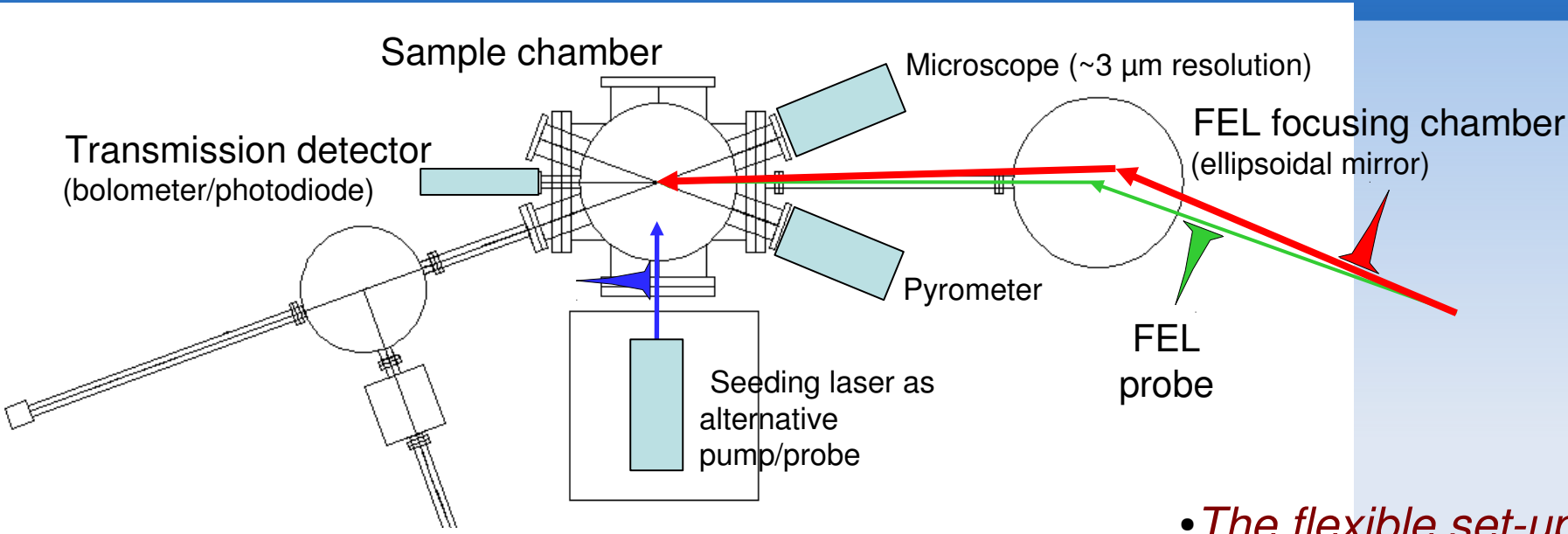

Journal of Non-Crystalline Solids 357 (2011) 2641–2647

Probing phase transitions under extreme conditions by ultrafast techniques: Advances at the Fermi@Elettra free-electron-laser facility

Andrea Di Cicco [a,b,c,*], Francesco D'Amico [b], Goran Zgrablic [b], Emiliano Principi [a], Roberto Gunnella [a],

Damage to VUV, EUV, and X-ray Optics III, edited by Libor Juha, Saša Bajt, Richard A. London,
Proc. of SPIE Vol. 8077, 807704 · © 2011 SPIE · CCC code: 0277-786X/11/$18 · doi: 10.1117/12.887633

Invited Paper

Probing matter under extreme conditions at FERMI@Elettra: the TIMEX beamline

Andrea Di Cicco[a], Filippo Bencivenga[b], Andrea Battistoni[b], Daniele Cocco[b], Riccardo Cucini[b], Francesco D'Amico[b], Silvia Di Fonzo[b], Adriano Filipponi[c], Alessandro Gessini[b], Erika Giangrisostomi[b], Roberto Gunnella[a], Claudio Masciovecchio[b], Emiliano Principi[b], and Cristian Svetina[b]

- *The flexible set-up of the Timex end-station can host different experimental configurations.*
- *Details on the experimental layout and pilot pump and probe experiments are reported in the papers of the Timex collaboration*

Set-up for first experiments

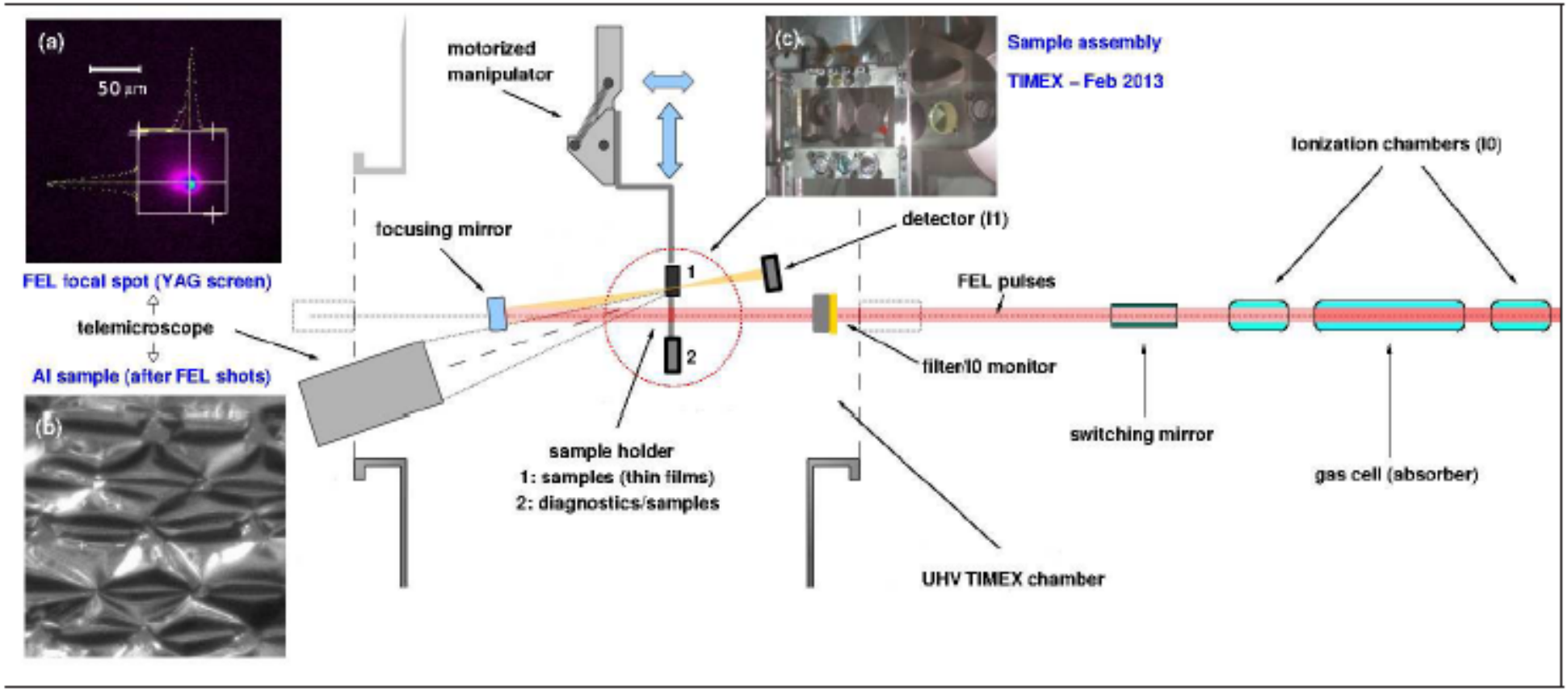

FIG. 1. Sketch of the experimental set-up including optics, diagnostics and detectors for transfer and control of the FEL pulses generated by the Fermi@Elettra FEL-1 source (right, not shown). From the right to the left (main figure) FEL pulses pass through ionization chambers (measuring the intensity I_0), a gas cell absorber (fluence reduction), a plane mirror and selected filters. In the left side we show the setup inside the UHV TIMEX chamber: the motorized manipulator holding sample and pulse diagnostics, the detector (photodiode measuring I_1), the focusing mirror, and the telemicroscope. Pictures (a), (b) and (c) show: (a) the FEL focal spot at sample position; (b) an image of the Al ultrathin sample surface after FEL pulse exposures; (c) the multi-sample assembly for this experiment.

Fluence and focusing

- Focusing provided by a spherical focusing mirror (metal or multilayer coating) with ~10x10 µm best focus size, (normal reflection: loss of about 90% of fluence for soft x-ray photons). The mirror was a platinum-coated silicon mirror (400 mm radius of curvature, 0.2 nm roughness RMS) placed close to normal incidence (angle of incidence 3 degs). Maximum fluence in these conditions was about 20 J/cm^2.

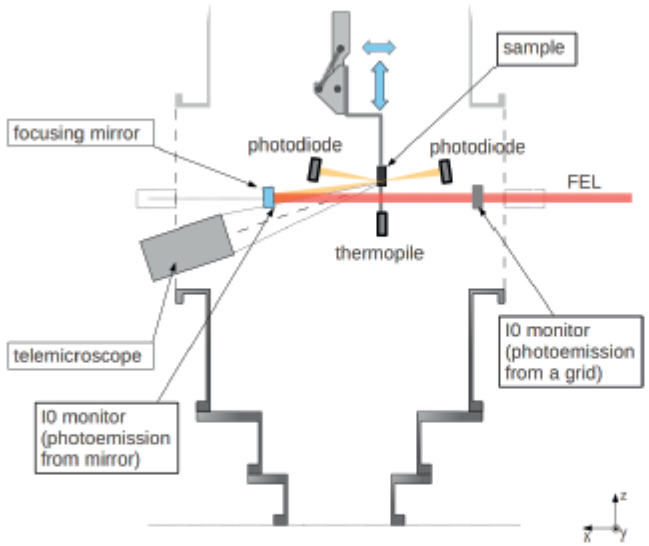

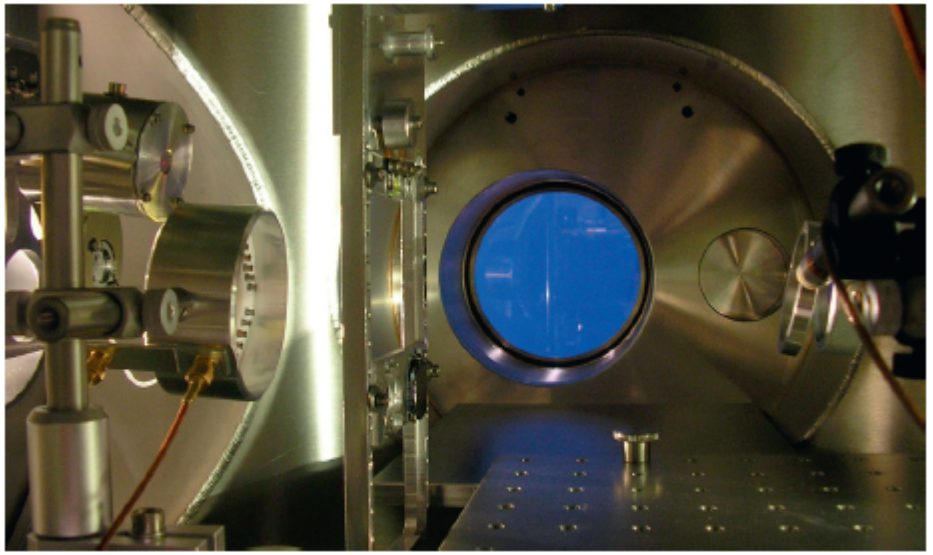

Figure 3

Left side: sketch of the current (March 2013) experimental set-up of the TIMEX chamber, including optics, detectors and diagnostics. Right side: picture of the setup including the sample holder (center), the Au grid (I_0 monitor) and a photodiode (left), and the focusing mirror (right).

Fermi pulses main features

•FERMI@Elettra seeded FEL user-facility. Two separate FEL amplifiers (FEL1 and FEL2) cover the spectral range from 100 nm (12eV) to 4 nm (320 eV), first harmonic. Based on the high gain harmonic generation scheme the two FEL provide photon pulses of about 100fs.

- ❑ high peak power — 0.3 – GW's range
- ❑ short temporal structure — sub-ps to 10 fs time scale
- ❑ tunable wavelength — var. gap APPLE II-type undulators
- ❑ variable polarization — horizontal/circular/vertical
- ❑ seeded harm. Cascade — strong long. and transv. coher.

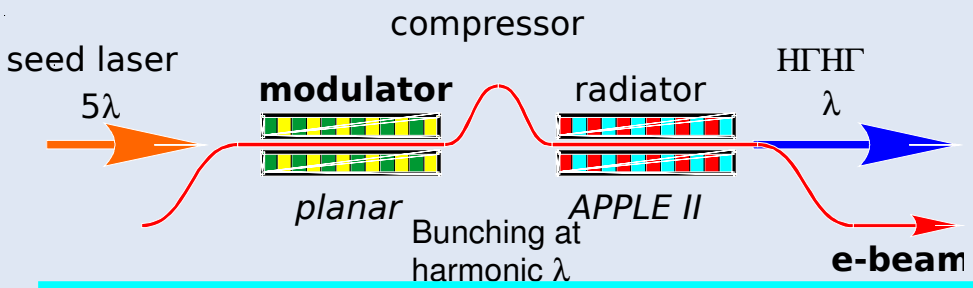

High Gain Harmonic Generation - HGHG

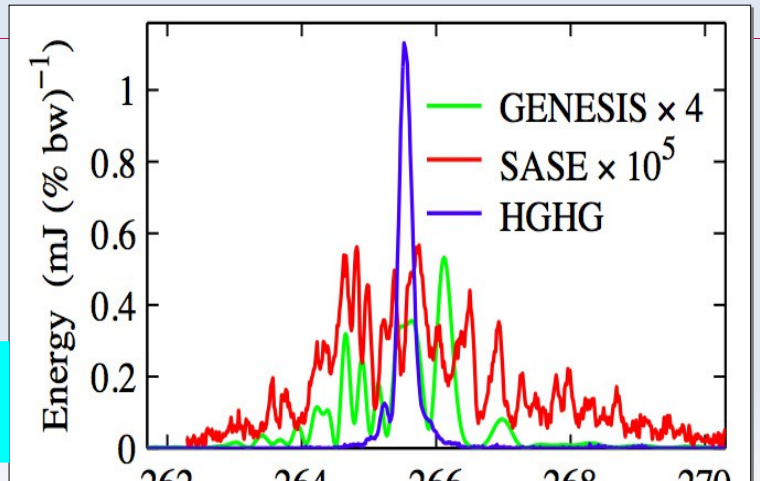

Li-Hua Yu
DUV-FEL,
Brookhaven

Shape of the pulse

Seeded laser

Energy space

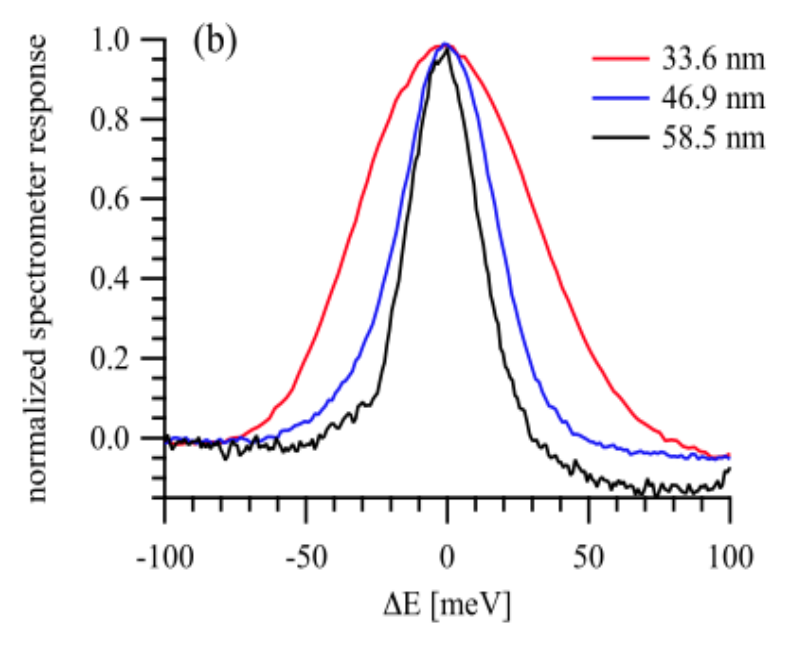

Real space

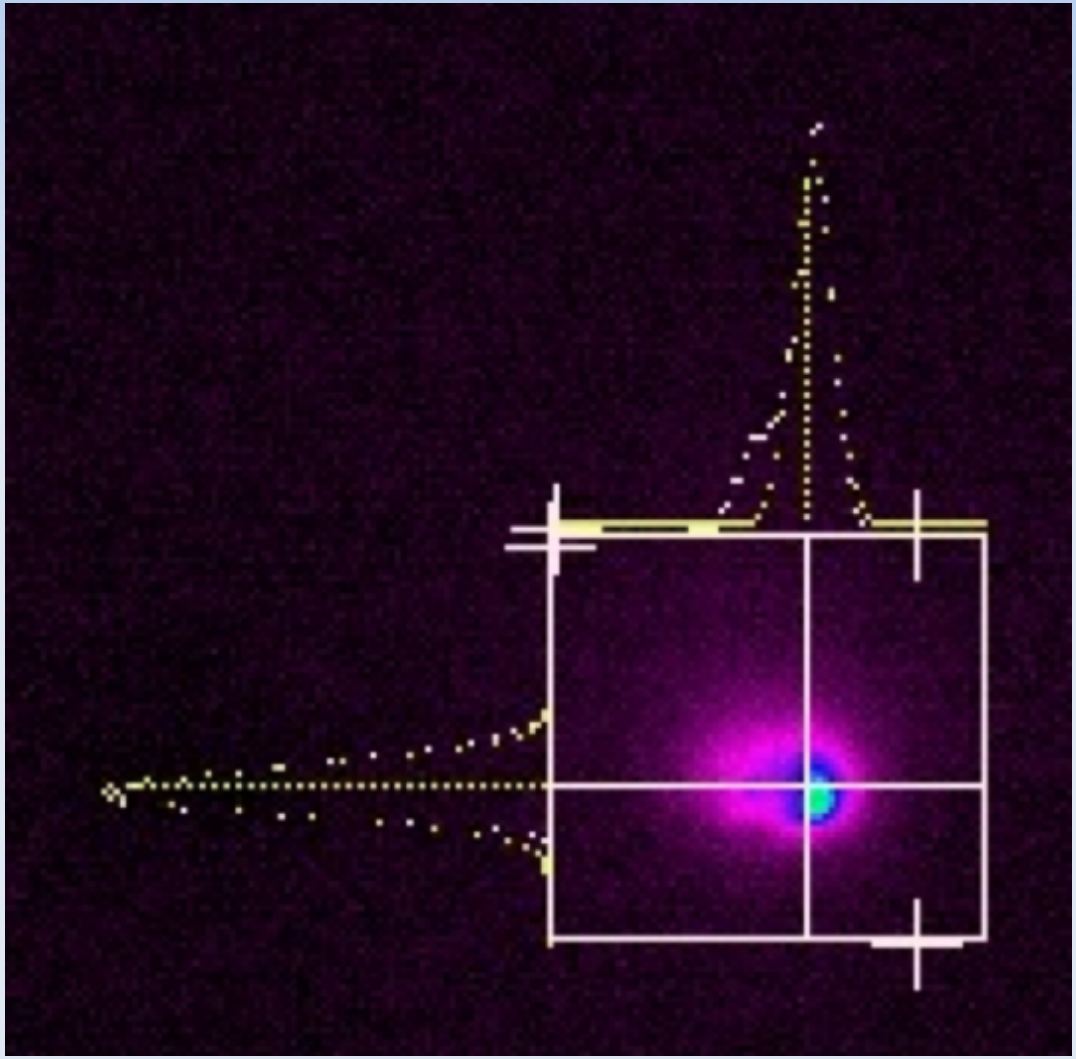

E. Allaria et. al., New J. Phys. (2012)

10x10 μ FWHM

Tunability across the edges

Tunability experiments at the FERMI@Elettra free-electron laser

- High-quality Ti $M_{2,3}$-edge (3p) absorption spectra with FEL1 ultrashort pulses: near-edge changes at high fluence (high-energy density). E. Principi et al. (2013).

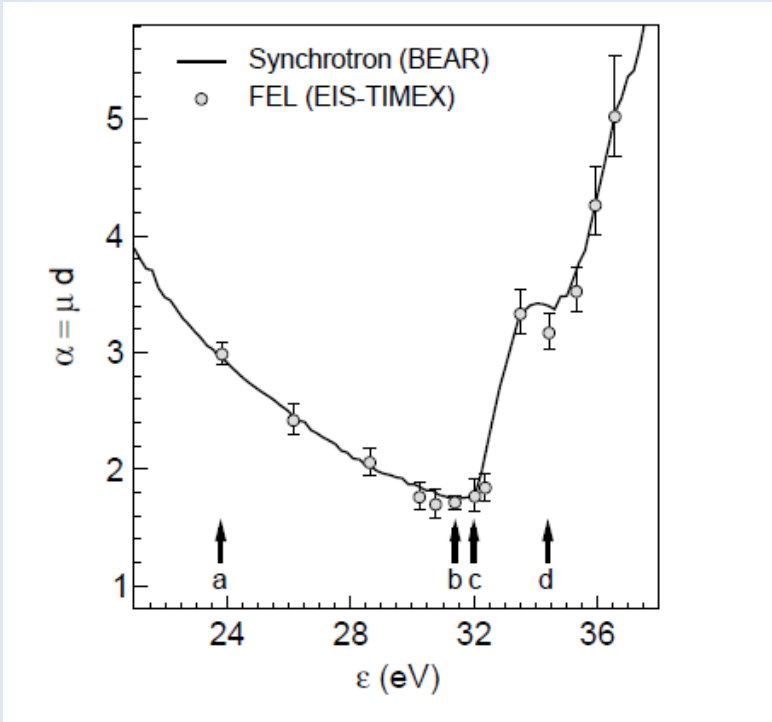

New Journal of Physics **14** (2012) 113009 (19pp)
Received 20 September 2012
Published 7 November 2012

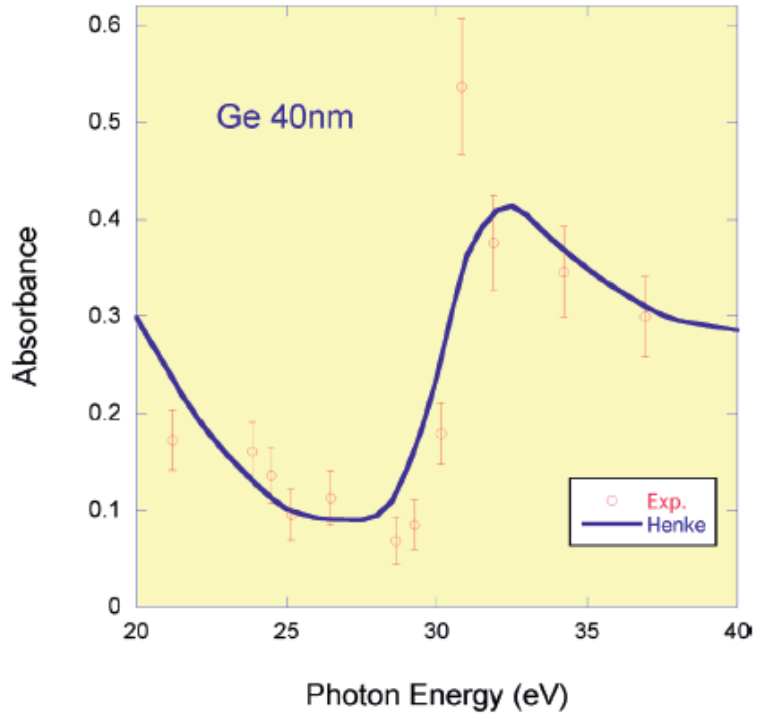

Figure 6

First near-edge $M_{4,5}$ x-ray absorption spectrum (dots with error bars) of a 40 nm Ge ultrathin foil collected at FERMI@Elettra,[2] compared with the calculated absorbance (blue line[17]).

Reflectivity increase in Ti

- New phenomenon observed in the range 18.9-20 eV, interpreted as a shift of the plasmon energy (Drude model, ~17 eV in Ti) as a consequence of the injection of free electrons (increase of the electron density) within the pulse duration.

$$\omega_p = \sqrt{N_e e^2 / m_e \epsilon_0},$$

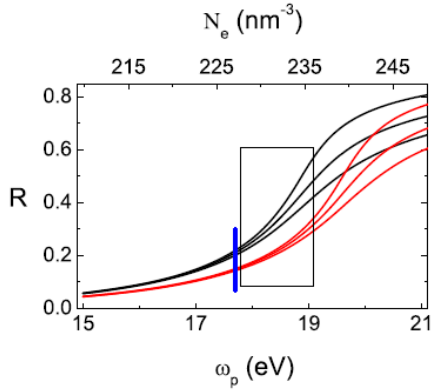

Figure 1 | $\hbar\omega_p$-dependence of R for $\hbar\omega$ = 18.9 and 20 eV (black/red lines) and $\hbar\gamma$ = 1, 1.5 and 2 eV (higher to lower curves), calculated with Eqs.(3) and (4); the upper horizontal scale is the corresponding range in N_e calculated through Eq. (1). The vertical blue segment indicates the expected value of $\hbar\omega_p = \hbar\omega_p(0) = 17.7$ eV for the unexcited Ti sample[27,28], while the hatched area sketches the $\hbar\omega_p$-range reached in the excited sample in the exploited F-range.

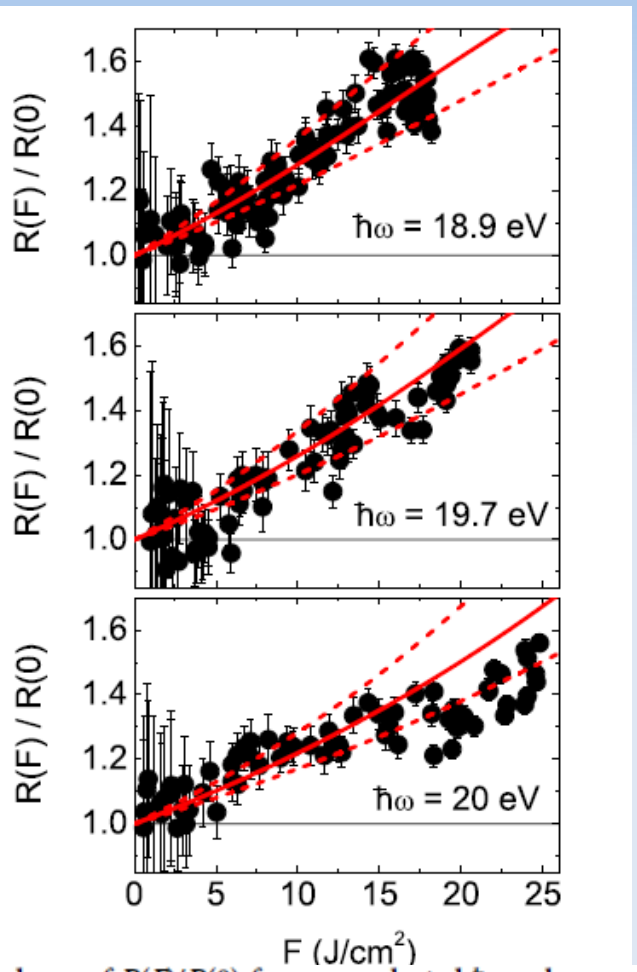

Figure 2 | F-dependence of $R(F)/R(0)$ for some selected $\hbar\omega$-values, indicated in the individual panels. Each data corresponds to a single shot measurement taken in a fresh portion of the sample. Red full lines are the $R(F)/R(0)$ trends calculated through Eq. (6); dashed lines are the estimate of the confidence interval.

SCIENTIFIC REPORTS | 4 : 4952 | DOI: 10.1038/srep04952

Saturable absorption – first evidence

nature physics

ARTICLES

PUBLISHED ONLINE: 26 JULY 2009 | DOI: 10.1038/NPHYS1341

Turning solid aluminium transparent by intense soft X-ray photoionization

Bob Nagler *et al.**

Saturable absorption is a phenomenon readily seen in the optical and infrared wavelengths. It has never been observed in core-electron transitions owing to the short lifetime of the excited states involved and the high intensities of the soft X-rays needed. We report saturable absorption of an L-shell transition in aluminium using record intensities over 10^{16} W cm^{-2} at a photon energy of 92 eV. From a consideration of the relevant timescales, we infer that immediately after the X-rays have passed, the sample is in an exotic state where all of the aluminium atoms have an L-shell hole, and the valence band has approximately a 9 eV temperature, whereas the atoms are still on their crystallographic positions. Subsequently, Auger decay heats the material to the warm dense matter regime, at around 25 eV temperatures. The method is an ideal candidate to study homogeneous warm dense matter, highly relevant to planetary science, astrophysics and inertial confinement fusion.

FLASH Hamburg (2009)

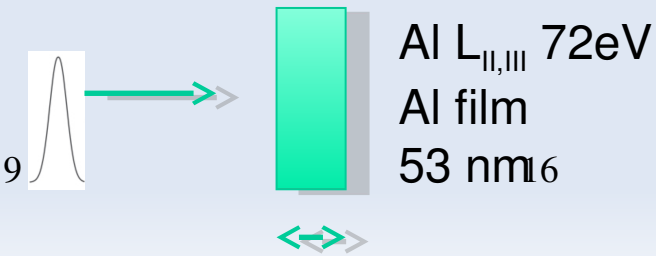

Transmission at high fluence

- Saturable absorption in Al observed at FLASH (Nagler et al., Nat. Phys. 5, 693–696 (2009) with 92 eV photon energy (15 fs pulse width). Al $L_{2,3}$-edges around 73 eV so the kinetic energy of photoelectron is about 20 eV. First TIMEX single-shot experiments at 23.7 eV (52.3 nm).

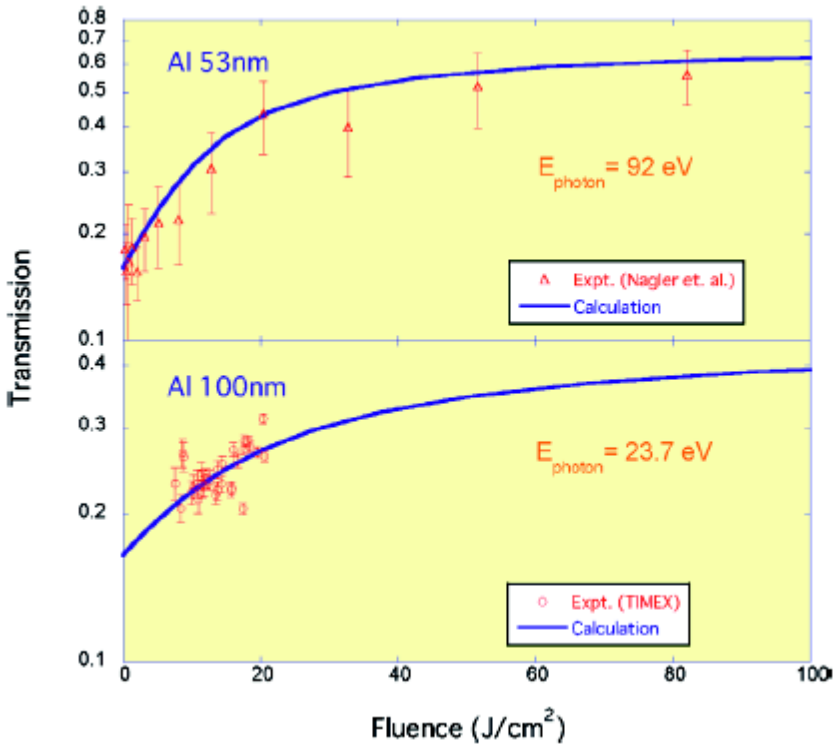

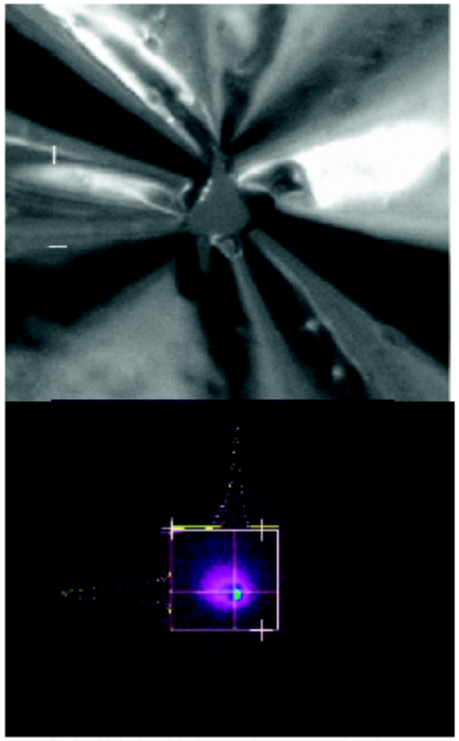

Figure 4

Left side: transmission of Al ultrathin foils as a function of the incident fluence of FEL pulses. The result of transmission measurements at the FLASH facility (see ref.[7]) and the first results obtained at TIMEX are compared with calculations (see text). Right side: the lower panel shows the lateral dimensions of the FEL pulses (10x10 μ FWHM) at focus (as observed on a YAG screen by the TIMEX telemicroscope), the upper panel shows the effect of about 100 repeated FEL shots (fluence 10-20 J/cm^2) on a 100 nm ultrathin Al foil. The pulses of seed laser were not filtered and concur to the damage of the foil.

Comparison with calculations

Modeling Non-Equilibrium Dynamics and Saturable Absorption Induced by Free Electron Laser Radiation

Keisuke Hatada *,† and Andrea Di Cicco

Journal of Electron Spectroscopy and Related Phenomena 196 (2014) 177–180

Appl. Sci. **2017**, *7*, 814; doi:10.3390/app7080814

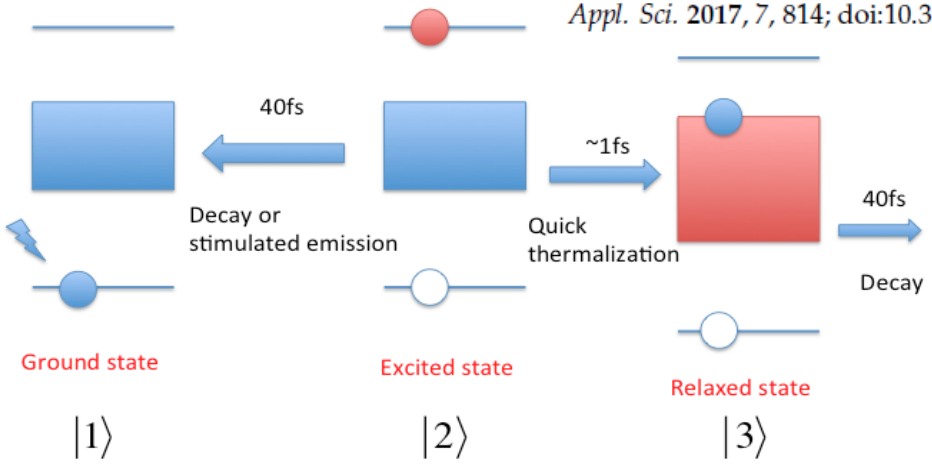

$$\frac{dN_1(z,t)}{dt} = \frac{a(z,t)I(z,t)}{\hbar\omega} + \frac{N_2(z,t)}{\tau_{21}} + \frac{N_3(z,t)}{\tau_{31}} \quad (1)$$

$$\frac{dN_2(z,t)}{dt} = -\frac{a(z,t)I(z,t)}{\hbar\omega} - \frac{N_2(z,t)}{\tau_{21}} - \frac{N_2(z,t)}{\tau_{23}} \quad (2)$$

$$\frac{dN_3(z,t)}{dt} = \frac{N_2(z,t)}{\tau_{23}} - \frac{N_3(z,t)}{\tau_{31}} \quad (3)$$

where

$$a(z,t) = \sigma\left(N_2(z,t) - \frac{d_2}{d_1}N_1(z,t)\right) \quad (4)$$

$$N = N_1(z,t) + N_2(z,t) + N_3(z,t) = const. \quad (5)$$

$$\frac{dI(z,t)}{dz} + \frac{1}{c}\frac{dI(z,t)}{dt} = a(z,t)I(z,t). \quad (6)$$

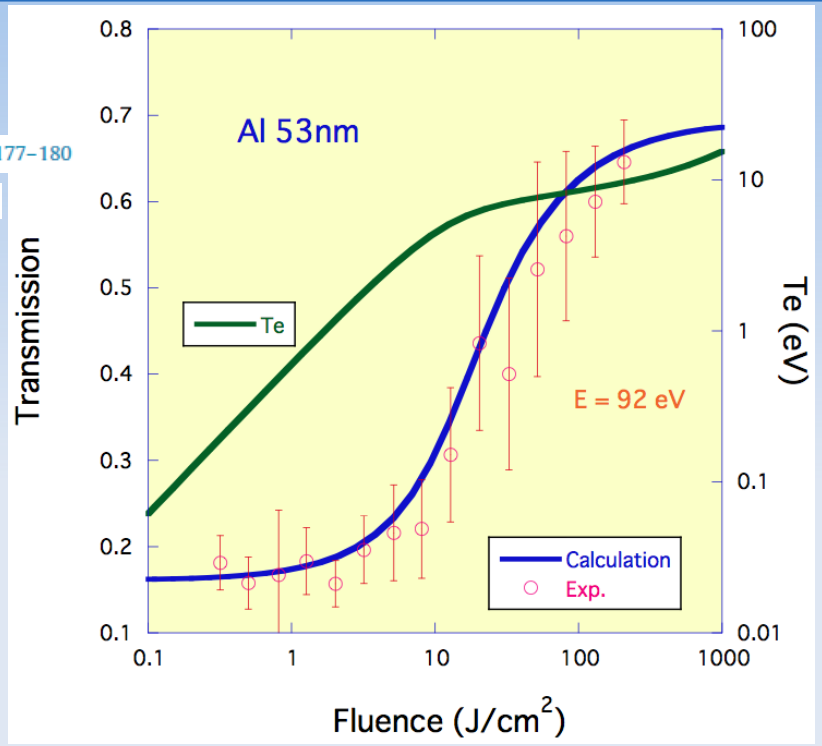

The photo-excited electrons have an energy of the order of 20 eV above the original Fermi energy. Measured inelastic scattering lengths for such electrons in aluminium are between 5 and 10 Å (ref. 21) corresponding to timescales of the order of 0.85–1.7 fs, in good agreement with calculations based on electron gas dielectric theory[22]. Thus, the photo-excited electrons rapidly lose their energy and thermalize with the initial cold valence electrons on a timescale considerably shorter than the FLASH pulse.

Electron thermalization

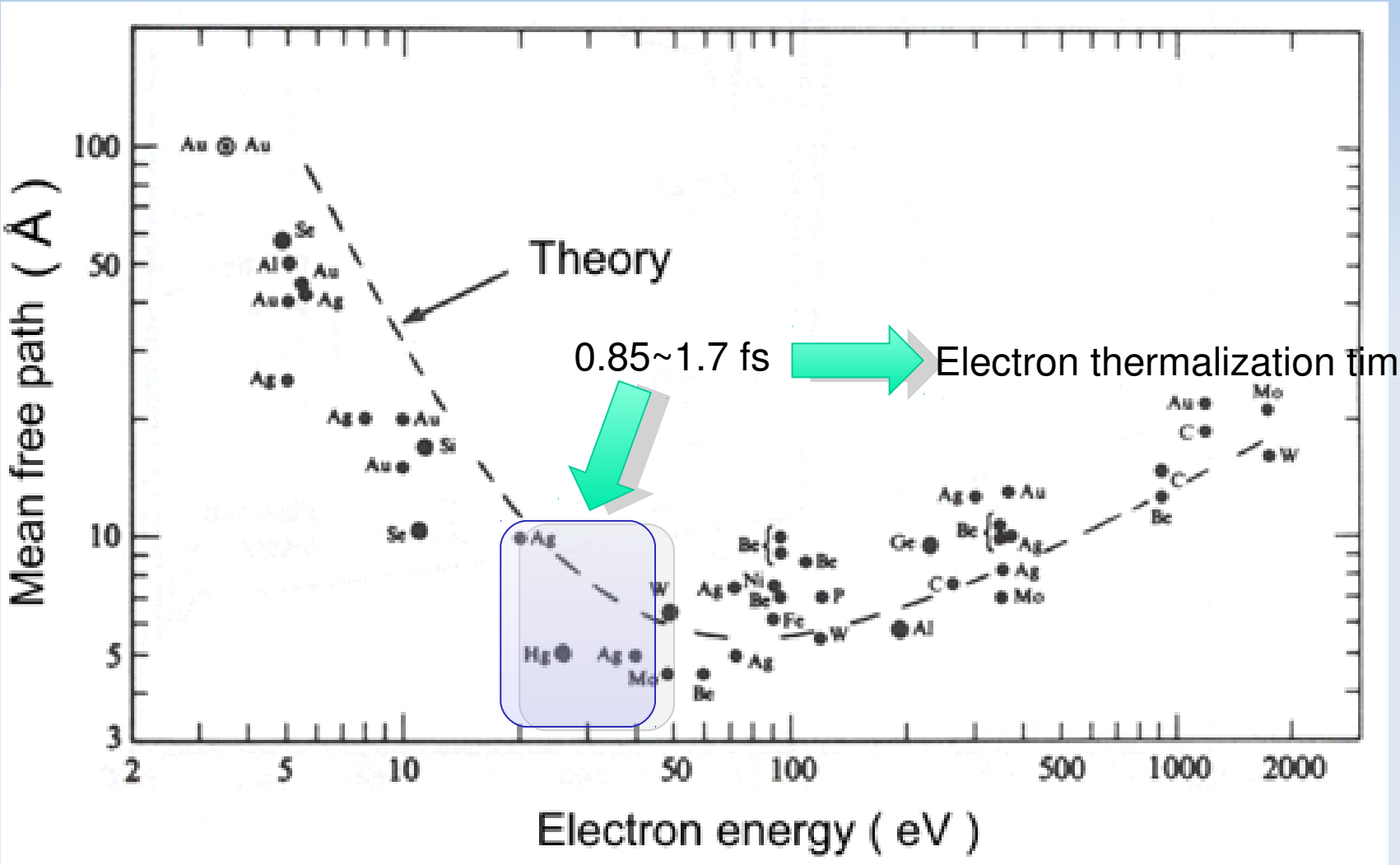

Fluence-dependent x-ray attenuation

- In the low fluence limit the attenuation is decreasing exponentially with the thickness (Lambert-Beer) while above the saturation threshold (about 1-10 J cm^{-2}) linearly.

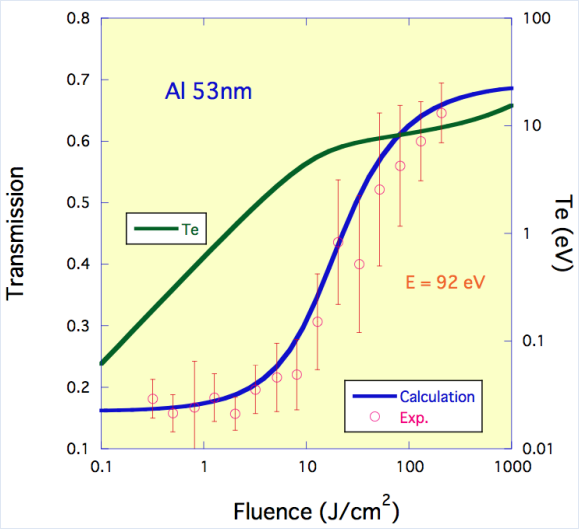

$$I = I_0 - a_0 I_{sat} z$$

Linear decay: (Non linear) Appropriate Homogeneous heating

$$I = I_0 e^{-a_0 z}$$

Exponential decay (Lambert-Beer)

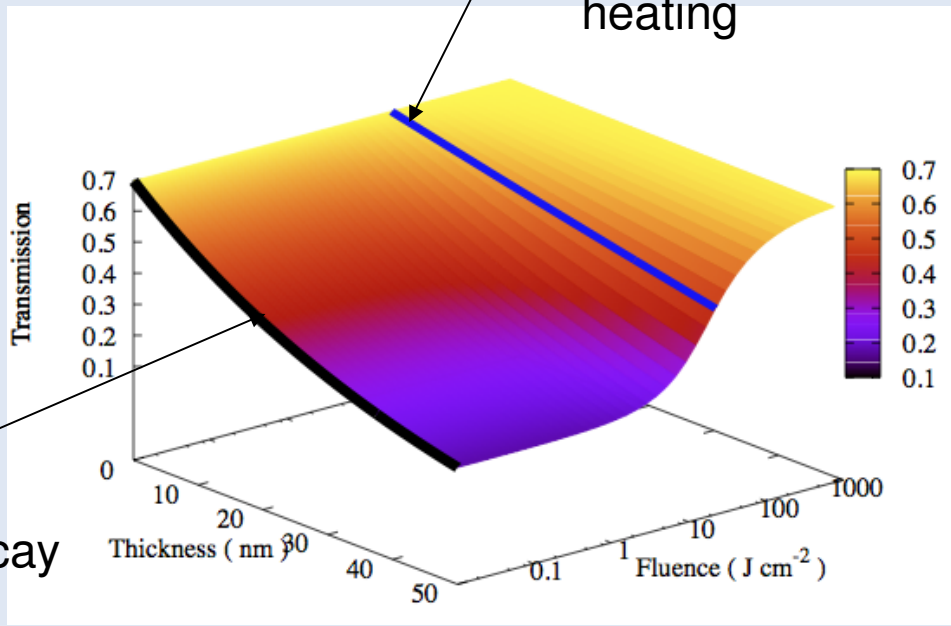

Ultrafast EUV transmission: experiments

- Measurement campaigns with different detectors and use of gas chamber/filters for fluence over 3 decades
- New observation: slightly decreasing transmittance (10%) at intermediate fluence (0.2-2 J/cm2), followed by a rise up to 10-20 J/cm2. on ultrathin 100 nm Al self-standing foils

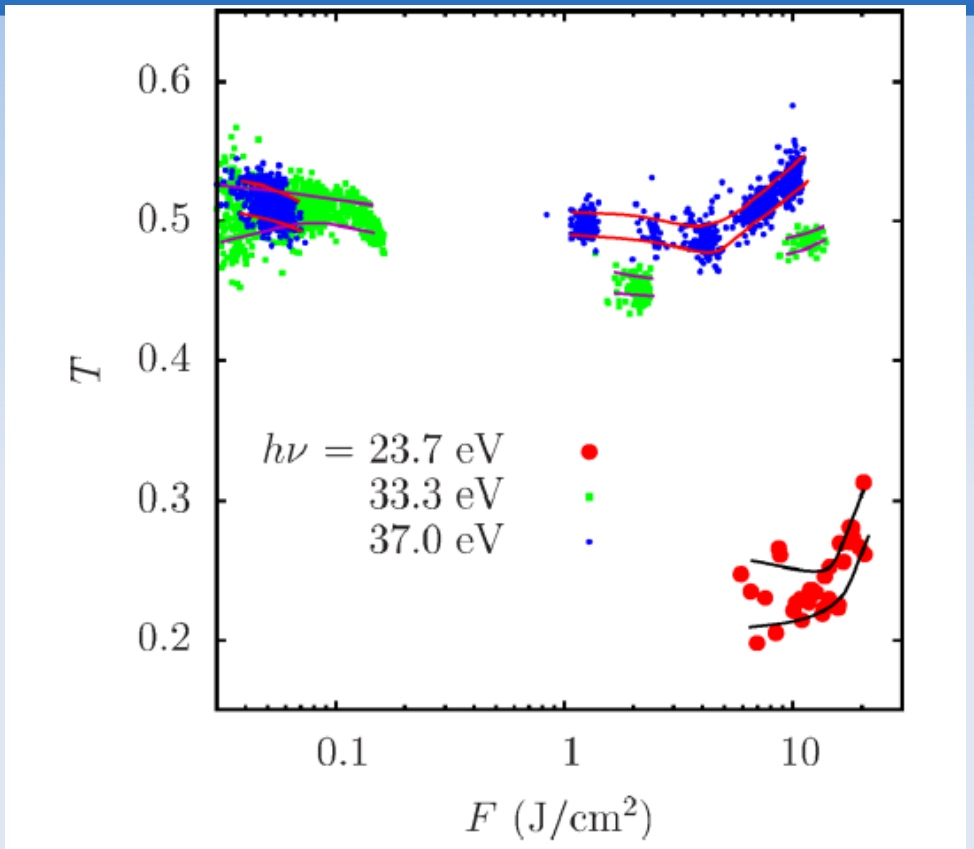

FIG. 2. (Color online) Single-shot transmission data of FEL-1 pulses across an ultrathin 100 nm Al foil as a function of the estimated fluence F. Data refer to a FEL photon energy of 23.7 eV (red circles), 33.3 eV (green squares), and 37.0 eV (blue circles). Lines depicted for each photon energy enclose bands of estimated uncertainty (standard deviation) for the single-shot data points within successive F intervals.

Nonlinear absorption of Al thin-film by EUV-FEL: electron heating

High Energy Density Physics 5 (2009) 124–131

Free–free opacity in warm dense aluminum

Sam M. Vinko[a,*], Gianluca Gregori[a], Michael P. Desjarlais[b], Bob Nagler[a], Thomas J. Whitcher[a], Richard W. Lee[c], Patrick Audebert[d], Justin S. Wark[a]

- Calculations (photon energy 30 eV) shows an increased opacity under different conditions while saturation effects start above 20 J/cm^2

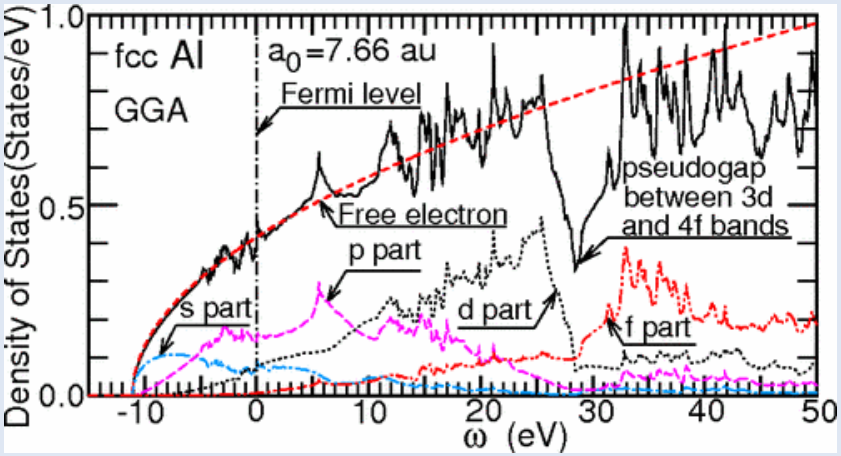

Takada PRL 2002

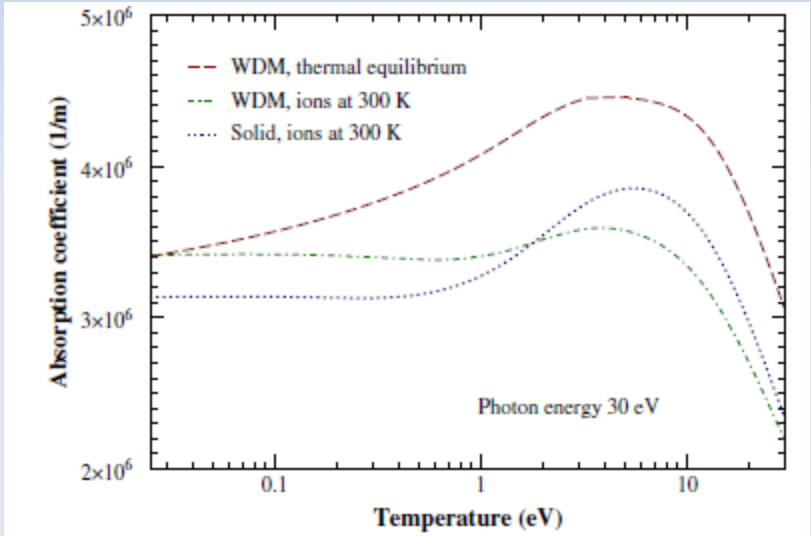

Fig. 8. Absorption coefficient versus temperature for warm dense Al in thermal equilibrium (red), warm dense Al with ions at room temperature (green) and solid Al with ions at room temperature (blue). Solid density and constant ionization $Z=3$.

Our pulse is ~100fs

Combining optical saturation and temperature effects for EUV absorption

PHYSICAL REVIEW B 90, 220303(R) (2014)

Interplay of electron heating and saturable absorption in ultrafast extreme ultraviolet transmission of condensed matter

High intensity pulses obtained by modern extreme ultraviolet (EUV) and x-ray photon sources allows thevobservation of peculiar phenomena in condensed matter. Experiments performed at the Fermi@Elettra FEL-1 free-electron-laser source at 23.7, 33.5, and 37.5 eV on Al thin films, for an intermediate-fluence range up tovabout 20 J/cm2, show evidence for a nonmonotonic EUV transmission trend. A decreasing transmission up tovabout 5–10 J/cm2 is followed by an increase at higher fluence, associated with saturable absorption effects. The present findings are interpreted within a simplified three-channel model, showing that an account of the interplay between ultrafast electron heating and saturation effects is required to explain the observed transmission trend.

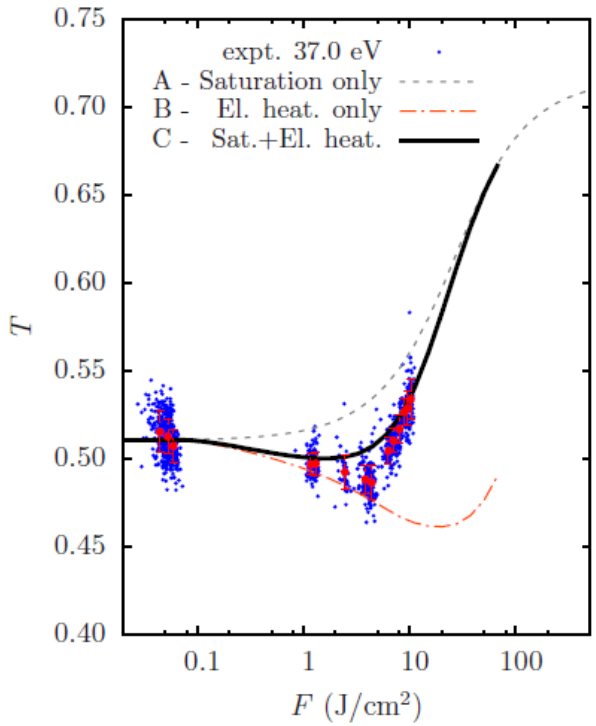

FIG. 3. (Color online) Experimental EUV transmission data compared with different calculations (see text). Curve *A* includes only optical saturation phenomena without accounting for temperature effects; curve *B* includes electron heating but neglects saturation phenomena; curve *C* takes into account both electron heating and saturation effects. The vertical bars refer to the average and standard deviations of single-shot data points within successive *F* intervals.

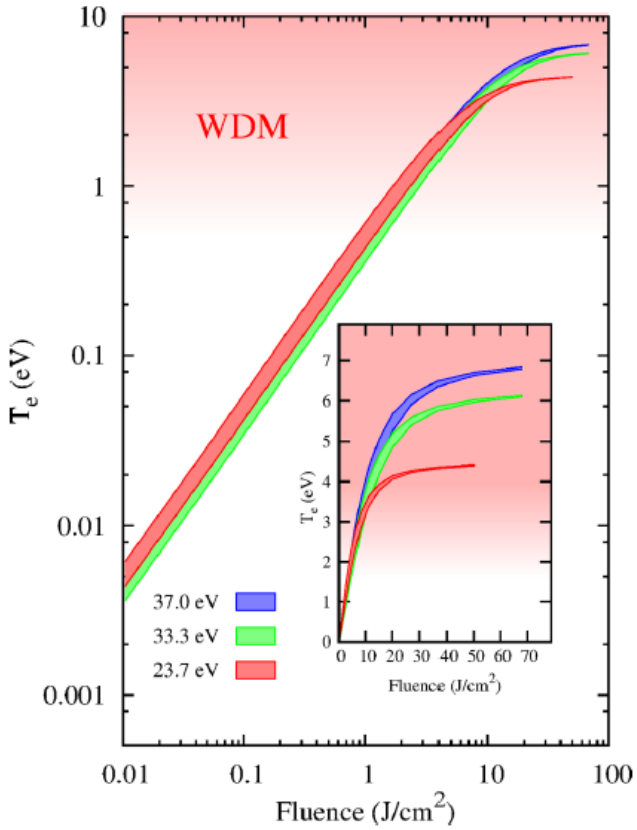

FIG. 4. (Color online) Estimated electron temperature in the 100 nm thick Al thin film as a function of incoming fluence at different FEL photon energies (curves enclose maximal and minimal temperatures through the film for given fluence). Electron temperatures in excess of 1 eV are obtained for fluence regimes above ~3 J/cm^2. Saturable absorption is found to limit the deposited energy above 10 J/cm^2 providing uniform bulk heating in the high-fluence regime (see the inset on a linear scale).

Optical saturation as a tool to reach bulk and homogenous Warm Dense Matter

1eV : 11604 K

Application of EUV/X-FEL to condensed matter. FEL pulses can heat the solid in very short time.

In saturation condition we can heat the material homogeneously

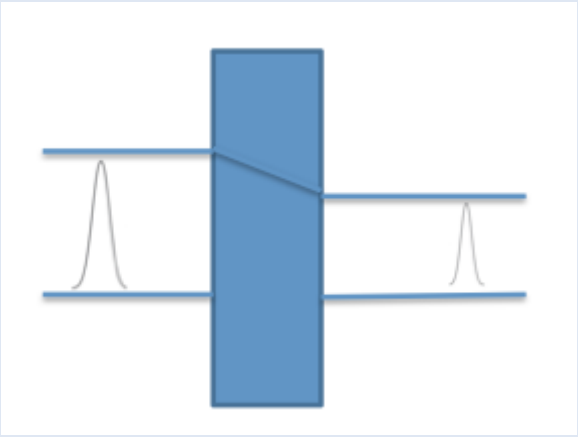

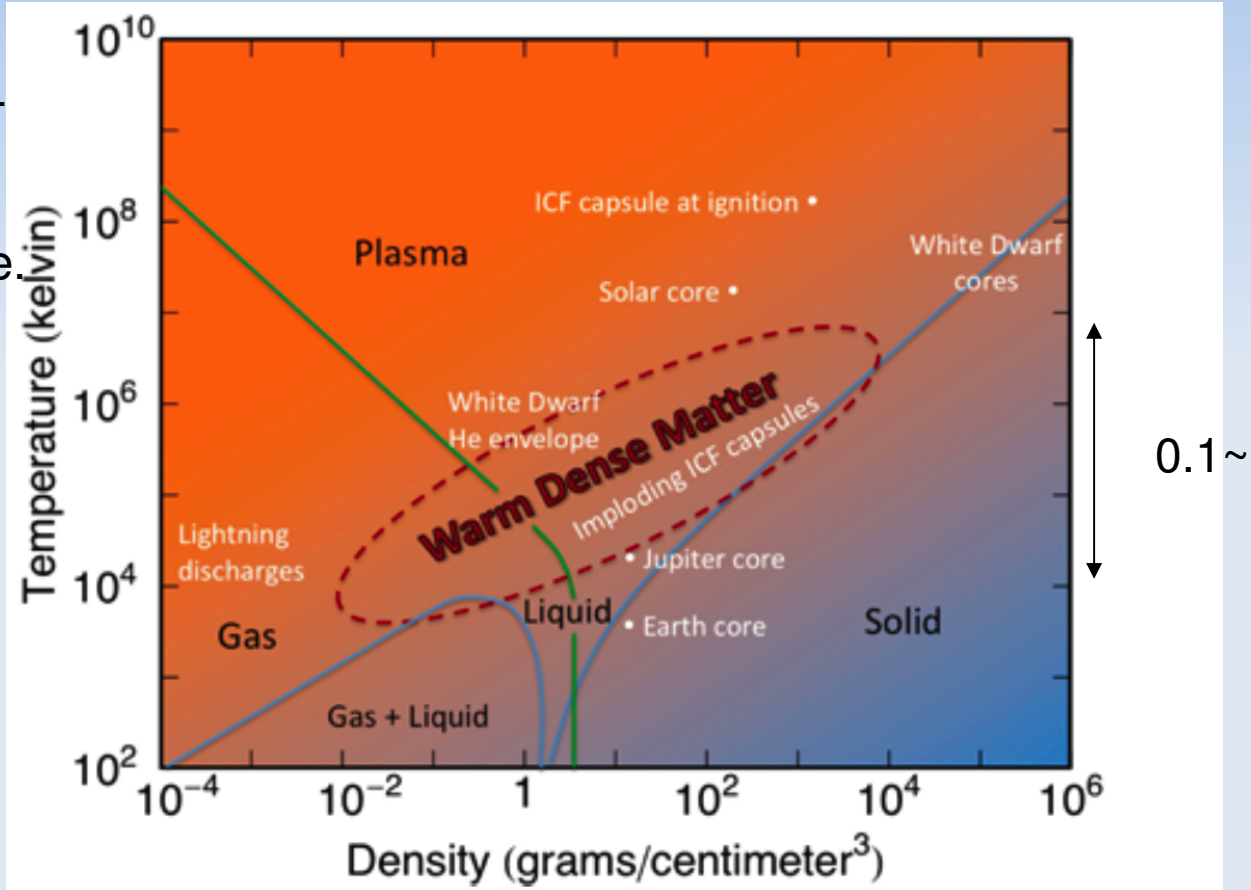

0.1~100 eV

Temperature versus density for various structures in the universe. Pressures corresponding to this temperature and density are between 100,000 and one billion atmospheres. Figure from "Basic Research Needs for High Energy Density Laboratory Physics," DOE Office of Science and NNSA (2010).

X-ray absorption for increased fluence

- Ti 3p near-edge ultrafast absorption data were collected for fluences up to about 10 Jcm-2 corresponding to electron temperatures in the 1-10 eV range.
- Clear changes in the shape at high fluence are assigned to ultrafast electron heating within 100 fs (no lattice heating)

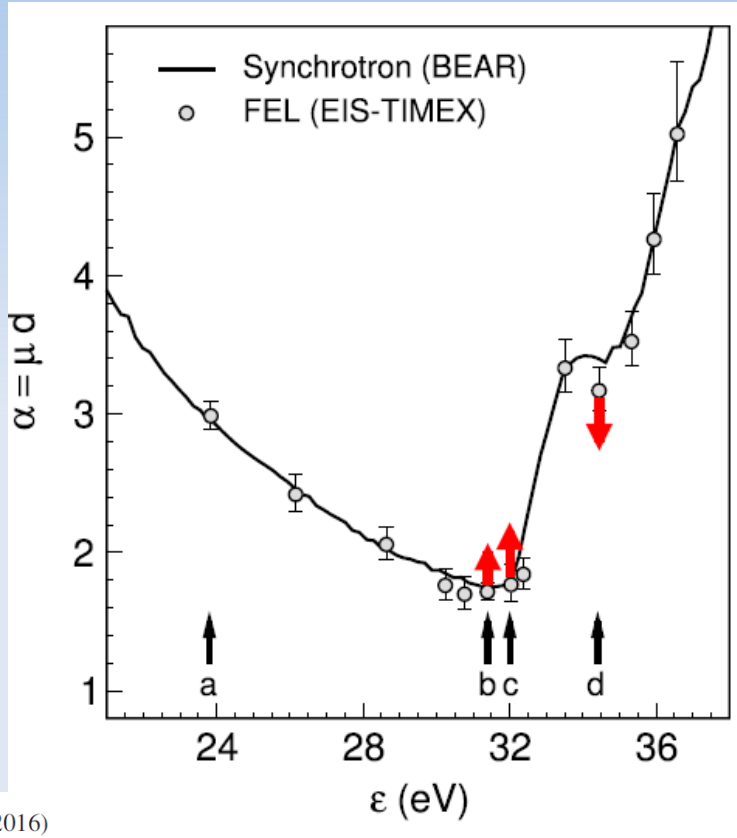

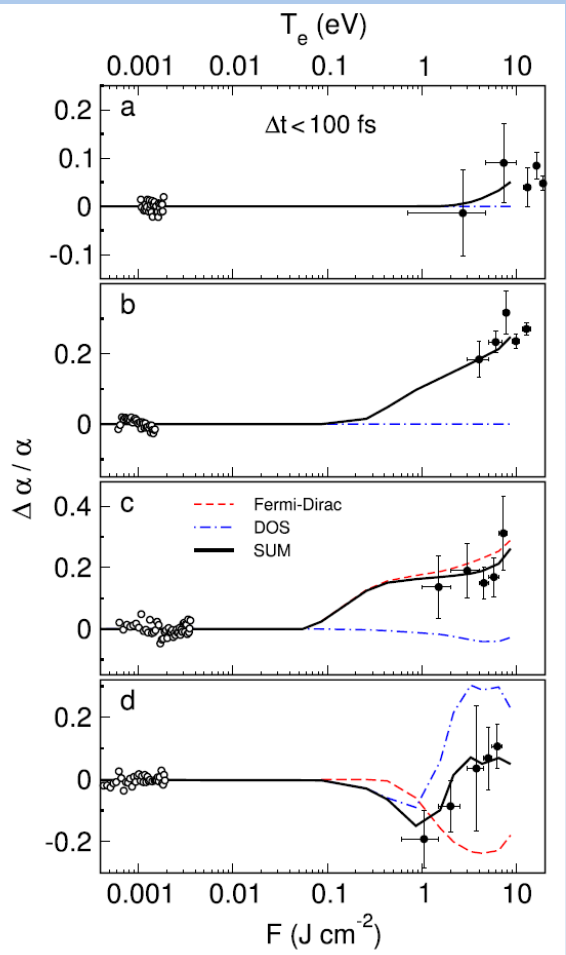

STRUCTURAL DYNAMICS **3**, 023604 (2016)

Free electron laser-driven ultrafast rearrangement of the electronic structure in Ti

E. Principi,[1,a)] E. Giangrisostomi,[1] R. Cucini,[1] F. Bencivenga,[1] A. Battistoni,[1] A. Gessini,[1] R. Mincigrucci,[1] M. Saito,[1] S. Di Fonzo,[1] F. D'Amico,[1] A. Di Cicco,[2] R. Gunnella,[2] A. Filipponi,[3] A. Giglia,[4] S. Nannarone,[4,5] and C. Masciovecchio[1,b)]

Pump&Probe: Pilot ultrafast experiments with a laser source

- Pump-and-probe reflectivity measurements on a fresh Si(100) surface. Laser source: pump at 400 nm, pulse width FWHM 80 fs, 500 Hz. Typical pump spot size 100 μm (pump) and 50 μm (probe).
- Super-continuum 350-800 nm probe, probing depth around 10 nm.

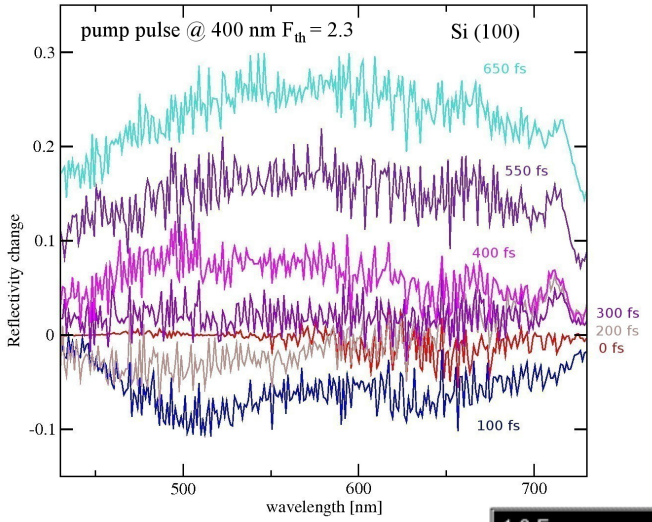

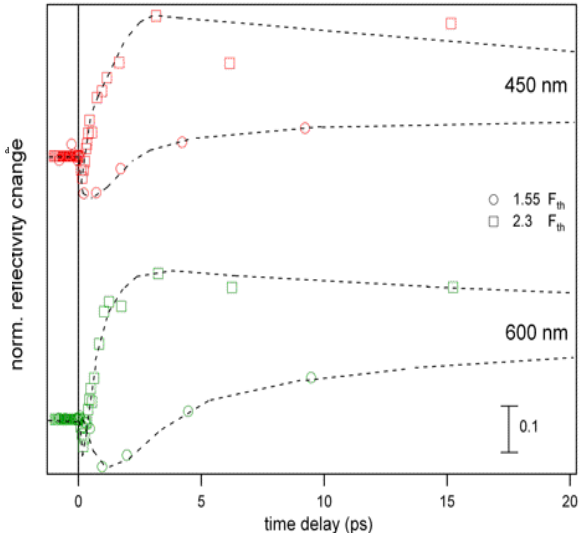

Journal of Non-Crystalline Solids 357 (2011) 2641–2647

Ultrafast pump-and-probe pilot reflectivity experiments on Si show that useful information about the dynamics of phase transitions can be obtained. Non-thermal melting of Si takes place within 300 fs and is followed by lattice heating or melting within 3 ps, as a function of the pump fluence.

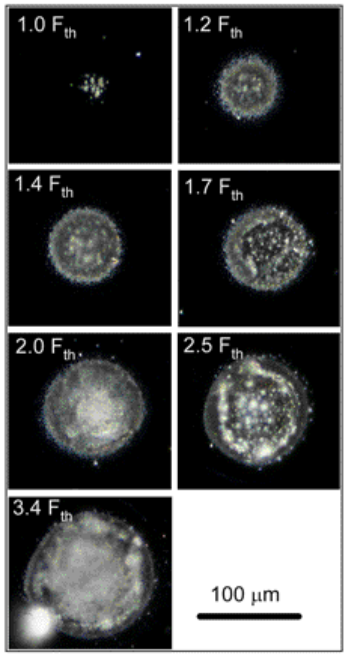

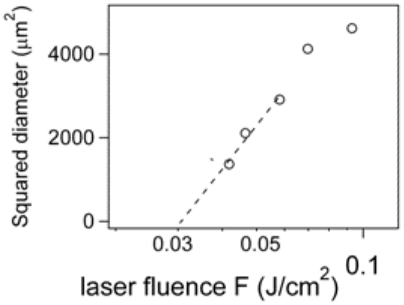

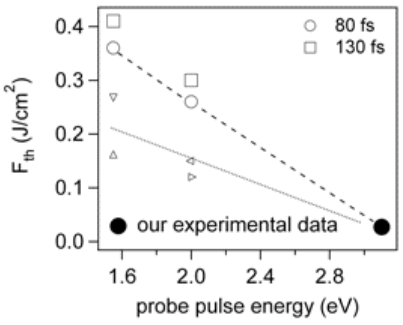

… more recent developments and needs

- Pump-probe experiments using the laser seed pulse (jitter-free, M. Danailov, Optics Express 22, 12869 2014) or a second FEL pulse (using a double-pulse mode or the delay line). Some experiments already done.
- Insertion of new detectors for x-ray emission. Tests and experiments done.
- General needs: Improvements in the diagnostics and detectors (including I0!).

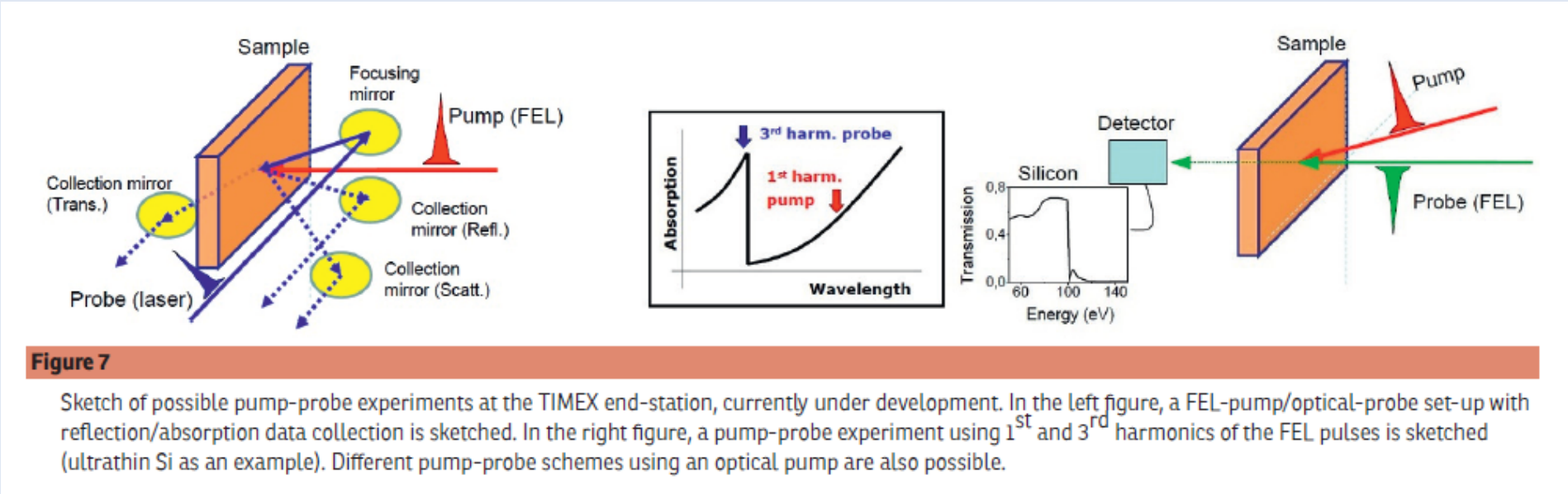

Figure 7

Sketch of possible pump-probe experiments at the TIMEX end-station, currently under development. In the left figure, a FEL-pump/optical-probe set-up with reflection/absorption data collection is sketched. In the right figure, a pump-probe experiment using 1st and 3rd harmonics of the FEL pulses is sketched (ultrathin Si as an example). Different pump-probe schemes using an optical pump are also possible.

Laser pump (167 nm)- FEL probe (40-65 eV): ultrafast carbon reflectivity

Photonics **2017**, *4*, 23; doi:10.3390/photonics4020023

Transient EUV Reflectivity Measurements of Carbon upon Ultrafast Laser Heating

Riccardo Mincigrucci *, Emiliano Principi, Filippo Bencivenga *, Laura Foglia, Alessandro Gessini, Gabor Kurdi, Alberto Simoncig and Claudio Masciovecchio

Elettra Sincrotrone Trieste SCpA, Basovizza, 34149 Trieste, Italy; emiliano.principi@elettra.eu (E.P.); laura.foglia@elettra.eu (L.F.); Alessandro.gessini@elettra.eu (A.G.); gabor.kurdi@elettra.eu (G.K.); alberto.simoncig@elettra.eu (A.S.); claudio.masciovecchio@elettra.eu (C.M.)

* Correspondence: riccardo.mincigrucci@elettra.eu (R.M.); filippo.bencivenga@elettra.eu (F.B.)

Received: 17 February 2017; Accepted: 18 March 2017; Published: 23 March 2017

Abstract: Time resolved extreme ultraviolet (EUV) transient reflectivity measurements on non-equilibrium amorphous carbon (a-C) have been carried out by combining optical and free electron laser (FEL) sources. The EUV probing was specifically sensitive to lattice dynamics, since the EUV reflectivity is essentially unaffected by the photo-excited surface plasma. Data have been interpreted in terms of the dynamics of an expanding surface, i.e., a density gradient rapidly forming along the normal surface. This allowed us to determine the characteristic time ($\tau \lesssim 1$ ps) for hydrodynamic expansion in photo-excited a-C. This finding suggests an extremely narrow time window during which the system can be assumed to be in the isochoric regime, a situation that may complicate the study of photo-induced metastable phases of carbon. Data also showed a weak dependence on the probing EUV wavelength, which was used to estimate the electronic temperature ($T_e \approx 0.8$ eV) of the excited sample. This experimental finding compares fairly well with the results of calculations, while a comparison of our data and calculations with previous transient optical reflectivity measurements highlights the complementarities between optical and EUV probing.

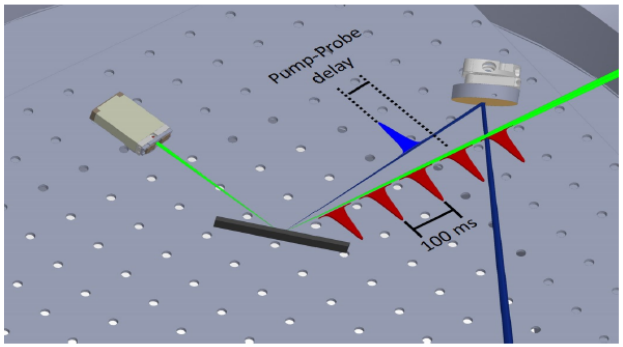

Figure 5. Sketch of the set-up in which the FEL pulses are separated by 100 ms. The first three FEL pulses probe the un-pumped reflectivity, while the last one probes the sample after the main pump–probe sequence. The blue pulse is the optical pump pulse which is time delayed with respect to the fourth FEL pulse.

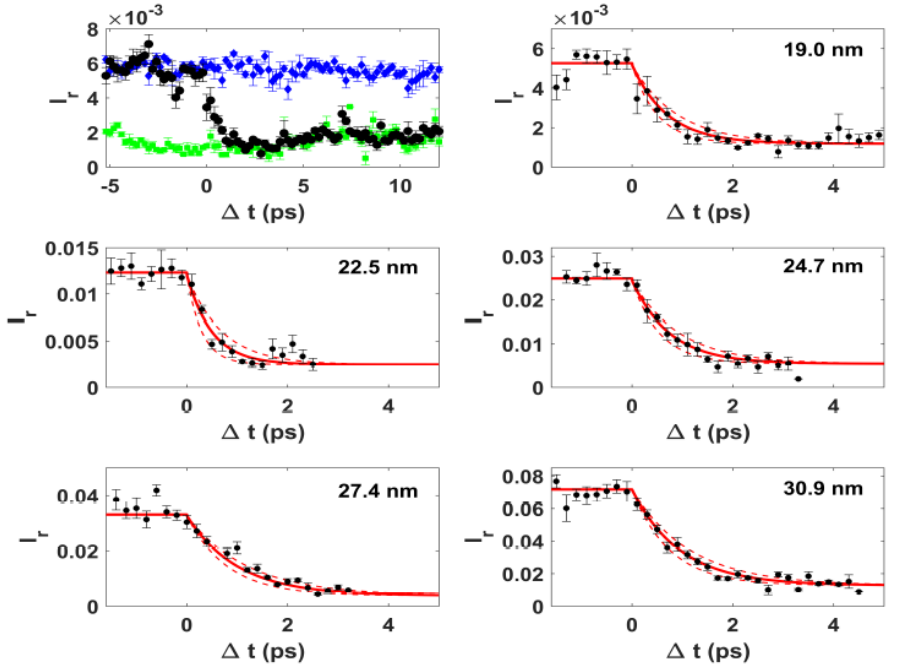

Figure 1. Top left: values of I_r recorded well before (more than 100 ms) the main pump–probe sequence (blue diamonds); at a given value of Δt after the optical pump pulse (black circles); and ~100 ms after the main pump–probe sequence (green squares). Data correspond to λ_{probe} = 19 nm. Other panels refer to the time resolved reflectivity change at the different free electron laser (FEL) wavelengths. Continuous lines are an exponential fit to data, while dashed lines are the confidence interval. Data have been scaled in order to match the tabulated extreme ultraviolet (EUV) reflectivity values [20] for negative Δt's.

The measurements have been carried out at the EIS-TIMEX beamline of the FERMI seeded FEL facility (Elettra, Trieste, Italy). The FEL pulses (time duration 70 fs full-width-half-maximum (FWHM), pulse energy 0.7 J) were focused on a 30 x15 µm2 spot size and spatially overlapped with the optical pump beam. The latter was a Ti:sapphire laser pulse frequency up-converted to the third harmonic (wavelength 260 nm, pulse duration 100 fs FWHM, pulse energy 45 J, spot size 70 x 100 µm2) and synchronized with the FEL pulse with a jitter less than 10 fs. The FEL probe wavelength (probe) was varied in the 19–31 nm spectral window. The sample was an a-C layer (70 nm thick) deposited on a Si substrate. The pulse energy of the pump pulse was large enough to induce, at least, the melting of the a-C sample. The employed parameters for the laser correspond to a fluence of 0.6 J/cm2 , roughly six times that needed to melt graphite.

Single-shot XAS at a soft x-ray SASE FEL: some news...

Normalized single-shot X-ray absorption spectroscopy at a free-electron laser

Vol. 44, No. 9 / 1 May 2019 / *Optics Letters* 2157

GÜNTER BRENNER,[1,*] SIARHEI DZIARZHYTSKI,[1] PITER S. MIEDEMA,[1] BENEDIKT RÖSNER,[2] CHRISTIAN DAVID,[2] AND MARTIN BEYE[1]

A setup for dispersive X-ray absorption spectroscopy (XAS), employing a new reference scheme, has been implemented and tested at the soft X-ray free-electron laser (FEL) FLASH in Hamburg. A transmission grating was used to split the FEL beam into two copies (signal and reference). The spectral content of both beams was simultaneously measured for intensity normalization within the FEL bandwidth on a shot-to-shot basis. Excellent correlation between the two beams was demonstrated within a few percent for single bunch operation at 143 eV photon energy. Applying the normalization scheme, an absorption spectrum of a Gd_2O_3 thin film sample was recorded around the Gd $N_{4,5}$-edge photon energy of 143 eV, showing excellent agreement with a reference spectrum measured at a synchrotron. This scheme opens the door for time-resolved single-shot XAS with femtosecond time resolution at FELs.

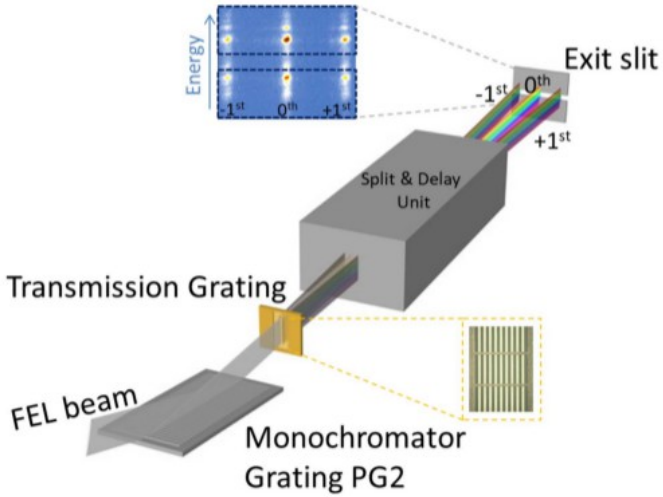

Fig. 1. Schematic of the setup for XAS at FLASH using a TG to split the FEL beam into a signal and reference beam (+1st and −1st order, respectively).

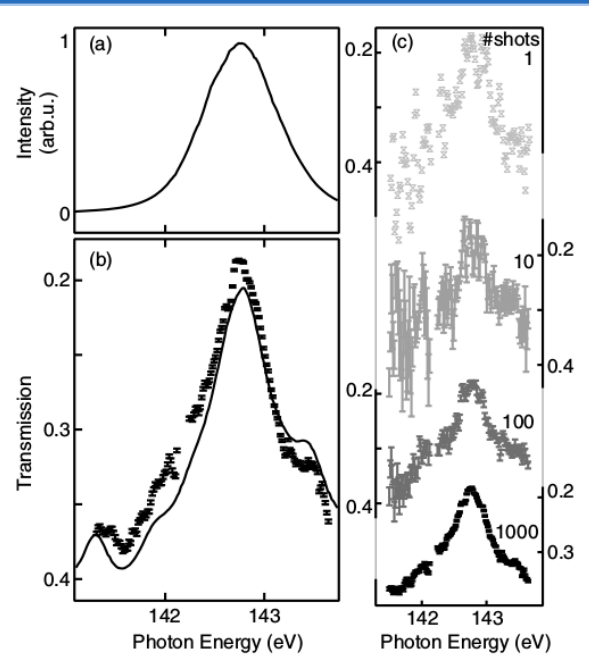

Fig. 5. (a) Average spectral distribution of FLASH. A total energy bandwidth of 0.9 eV FWHM was measured. (b) Gd $N_{4,5}$-edge x-ray absorption spectrum measured in transmission of a Gd_2O_3 thin film. The symbols represent data recorded at FLASH, while the solid line displays a reference measurement of the sample from a synchrotron. (c) Single-shot and averaged spectra for 10, 100, and 1000 FEL pulses.

- Known problems: energy resolution better than the ~1% FEL bandwidth (grating mono) and normalization on a shot-to-shot basis (spikes and FEL intensity fluctuations).

Conclusions – Thank you!

1. FEL sources open new opportunities for investigating extreme and non-equilibrium states in condensed matter. The XAS technique is shown to be particularly useful and ultrafast single-shot are possible.
2.Present results at the available EUV and soft x-ray facilities show that challenging single-shot XAS experiments can be done also using pump-probe schemes. Proper diagnostics for sample control and data normalization for XAS is still under development.
3. The realization of challenging XAS experiments at the new Eupraxia facility would need a dedicated beamline including diagnostics and solutions carried out in other FEL facilities.

Additional slides

P&P set-up: Time resolved optical spectroscopy

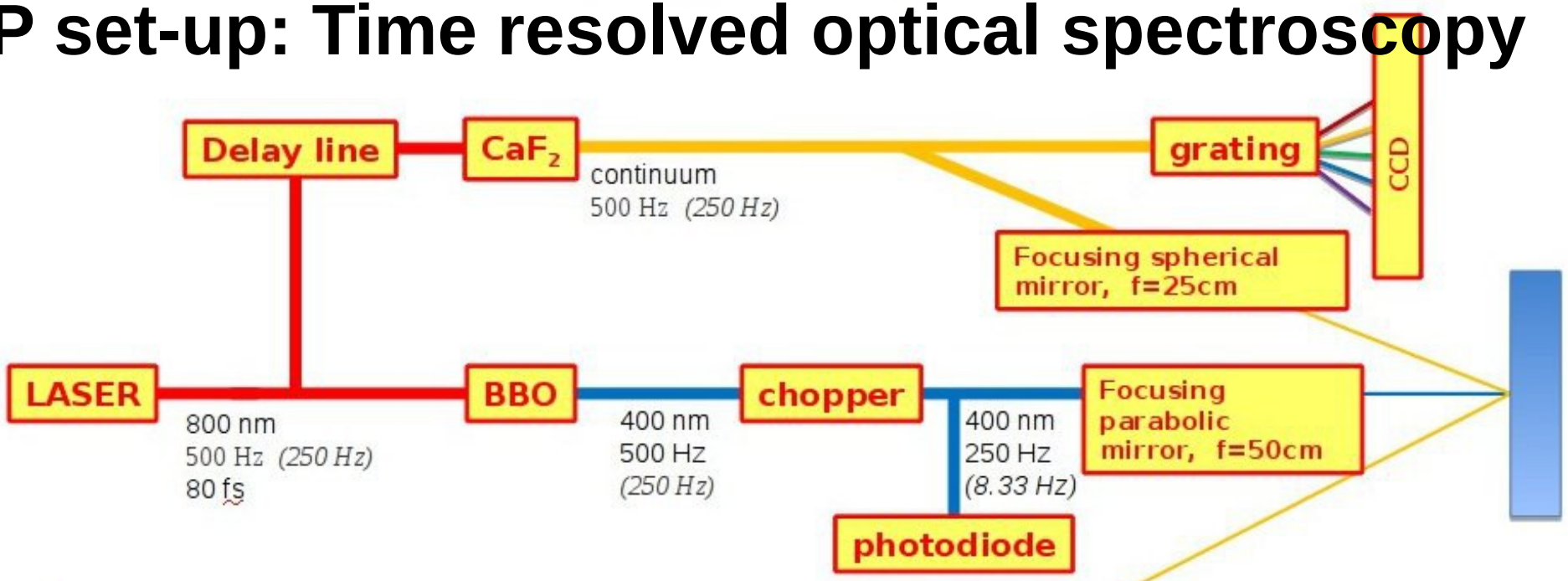

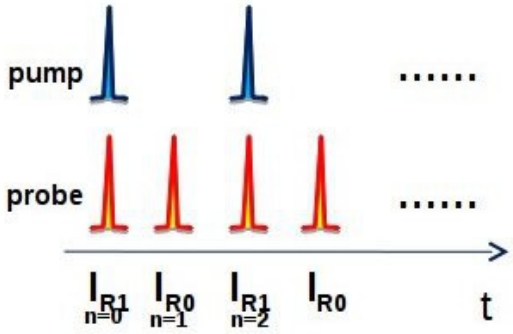

Normal repetition rate

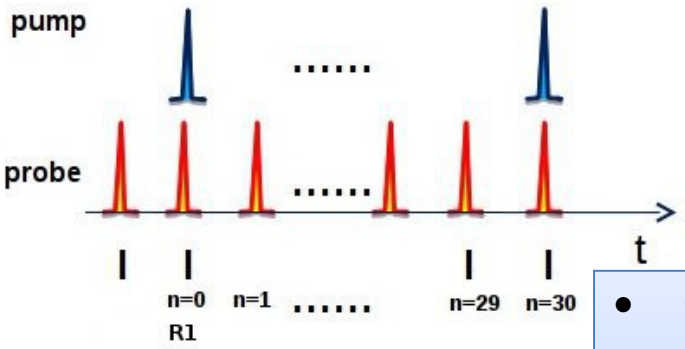

Single-shot configuration

Amplified Ti:Sapphire laser source: 800 nm, 80 fs, 2W, 1 kHz.

- transient transmittance (absorbance) or reflectivity of the sample
- 50 fs/3 nm time/spectral resolution, spectral range 350 – 1000 nm
- shot-to-shot detection, $<10^{-3}$ OD sensitivity
- observing in real-time the non-equilibrium dielectric function

Previous ultrafast experiments

·Si has an indirect gap (1.12 eV) so excitation with lasers with wavelengths λ > 364 Ang. Involve multi-photon and phonon-assisted transitions.

· At low laser fluencies a moderate negative change of the reflective was obtained.

·A positive reflectivity change within 200 fs is observed at high fluencies using P&P ultrafast techniques..

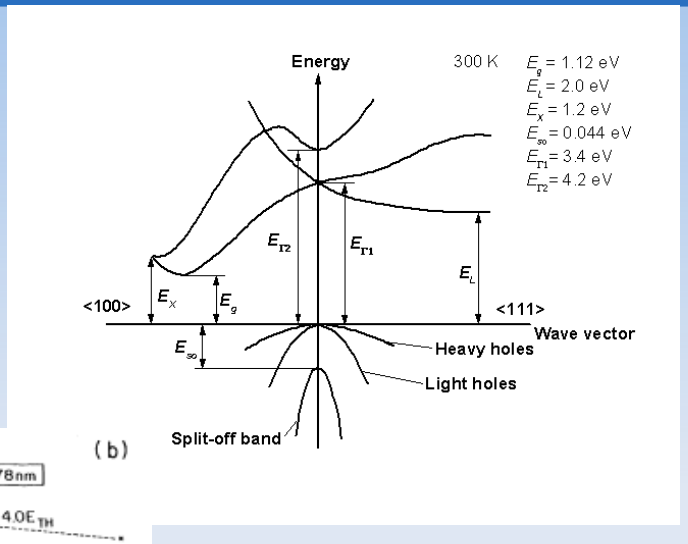

VOLUME 50, NUMBER 6 PHYSICAL REVIEW LETTERS 7 FEBRUARY 1983

Time-Resolved Reflectivity Measurements of Femtosecond-Optical-Pulse–Induced Phase Transitions in Silicon

C. V. Shank, R. Yen, and C. Hirlimann
Bell Telephone Laboratories, Holmdel, New Jersey 07733
(Received 29 November 1982)

The reflectivity of silicon has been measured following excitation with intense 90-fsec optical pulses. These measurements for the first time clearly resolve in time the process of energy transfer to the crystal lattice and the dynamics of the phase transition to the melted state.

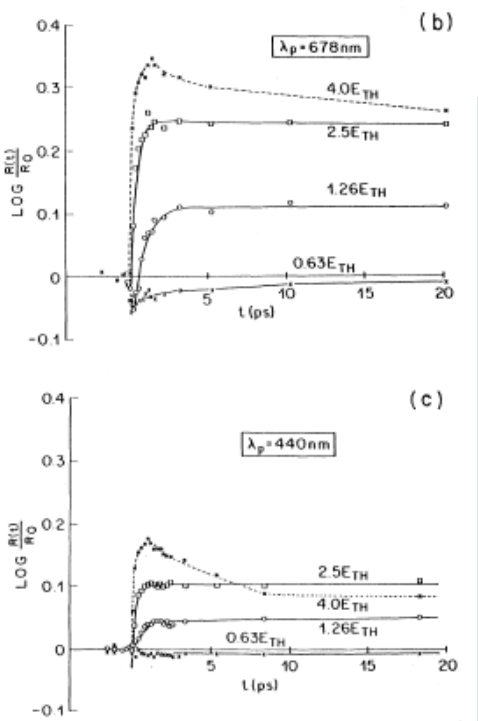

FIG. 1. Transient reflectivity data at three probe wavelengths following a 90-fsec excitation pulse at 620 nm. The solid lines for the $0.63E_{th}$ data are calculated on the basis of carrier diffusion into the bulk. The solid lines $E \geq E_{th}$ are calculated with the thin-film melting model. The dashed curves at the highest excitation are to guide the eye.

PHYSICAL REVIEW B VOLUME 61, NUMBER 4 15 JANUARY 2000-II

Generation of dense electron-hole plasmas in silicon

K. Sokolowski-Tinten and D. von der Linde
Institut für Laser- und Plasmaphysik, Universität-GHS-Essen, D-45117 Essen, Federal Republic of Germany

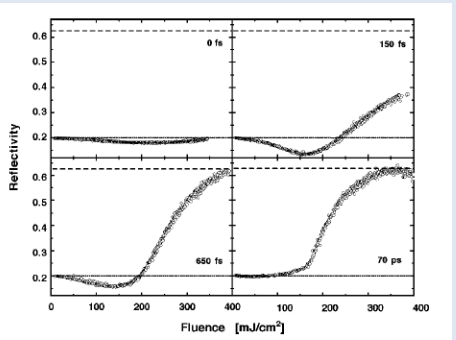

FIG. 2. Reflectivity of silicon as a function of excitation fluence for four different delay times, 625-nm wavelength, 49° angle of incidence, and *p* polarization. The dotted and dashed lines mark the reflectivity of solid and liquid silicon, respectively.

Non-thermal melting

·The positive reflectivity change is associated with a rapid melting process.

·The sudden laser-induced excitation of a large fraction of valence electrons into the conduction band changes the potential energy landscape.

· Tight-binding calculations show that the minimum associated with the diamond structure becomes a saddle point and within 100 fs atoms are displaced of about 1 Ang. (15% valence electron plasma) with average increase of temperature around 0.3 eV leading to melting (critical density estimated around 10^{22} cm $^{-3}$)

·The dramatical ultrafast weakening of the bond is confirmed by ab-initio MD calculations predicting a metallic liquid within 100-200 fs.

PHYSICAL REVIEW B VOLUME 49, NUMBER 11 15 MARCH 1994-I

Time dependence of the laser-induced femtosecond lattice instability of Si and GaAs: Role of longitudinal optical distortions

P. Stampfli* and K. H. Bennemann
Theoretical Physics, Freie Universität Berlin, Arnimallee 14, D-14195 Berlin, Germany

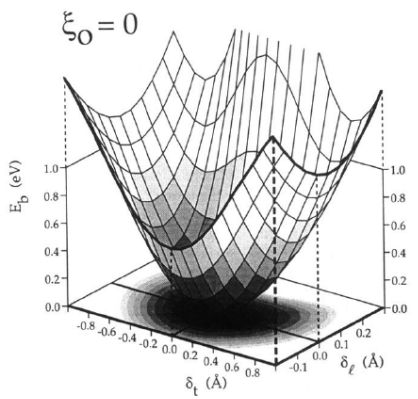

FIG. 2. Cohesive energy per atom E_b of Si [Eqs. (1)–(5)] in the absence of an electron-hole plasma (ξ_0=0) shown as a function of the transverse acoustic distortion δ_t and the longitudinal optical distortion δ_l of the diamond lattice. Here the ideal diamond structure (δ_t=δ_l=0) is a stable minimum of the cohesive energy.

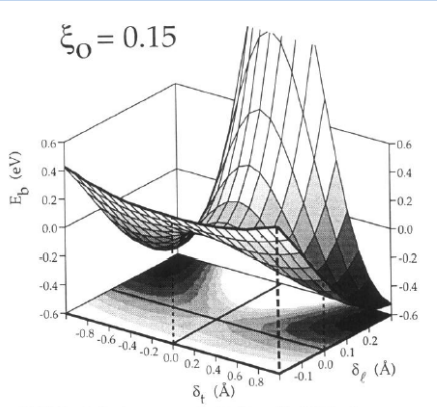

FIG. 3. Cohesive energy for Si [Eqs. (1)–(5)] in the presence of an electron-hole plasma of density ξ_0=0.15 corresponding to the excitation of 15% of the valence electrons into the conduction band. We use the same representation as in Fig. 2. Note that the ideal diamond structure (δ_t=δ_l=0) has become an unstable saddle point.

VOLUME 77, NUMBER 15 PHYSICAL REVIEW LETTERS 7 OCTOBER 1996

***Ab initio* Molecular Dynamics Simulation of Laser Melting of Silicon**

Pier Luigi Silvestrelli,[1] Ali Alavi,[2] Michele Parrinello,[1] and Daan Frenkel[3]

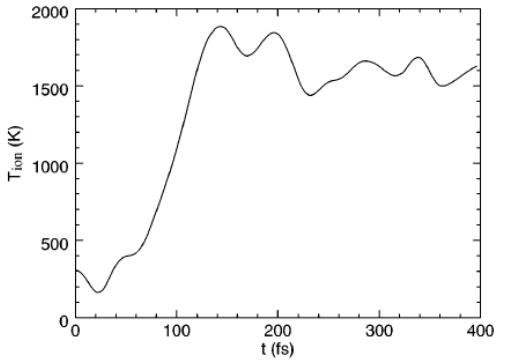

FIG. 1. Time dependence of the instantaneous ionic temperature, defined as $T_{\rm ion}(t) = [M/(3N-3)k_B]\sum_{I=1}^{N} v_I^2(t)$, where k_B is the Boltzmann constant, M is the Si ion mass, and $v_I(t)$ the ionic velocity at time t.

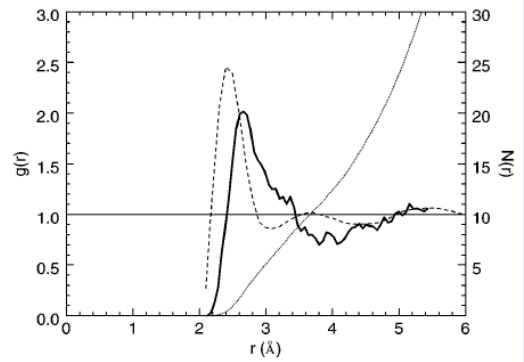

FIG. 3. Pair correlation function $g(r)$. Solid line: MD simulation. Dashed line: experimental result [19] for l-Si. Dotted line: coordination number $N(r)$.

Damage threshold

Summary of the electronic and structural effects after excitation with short laser pulses (direct-gap GaAs). Excitations range from 0.1 to 2.0 kJ m-2 . Three shaded regions indicate three distinct regimes.

From *S. K. Sundaram and E. Mazur, Nat. Mat. 1, 217 (2002).*

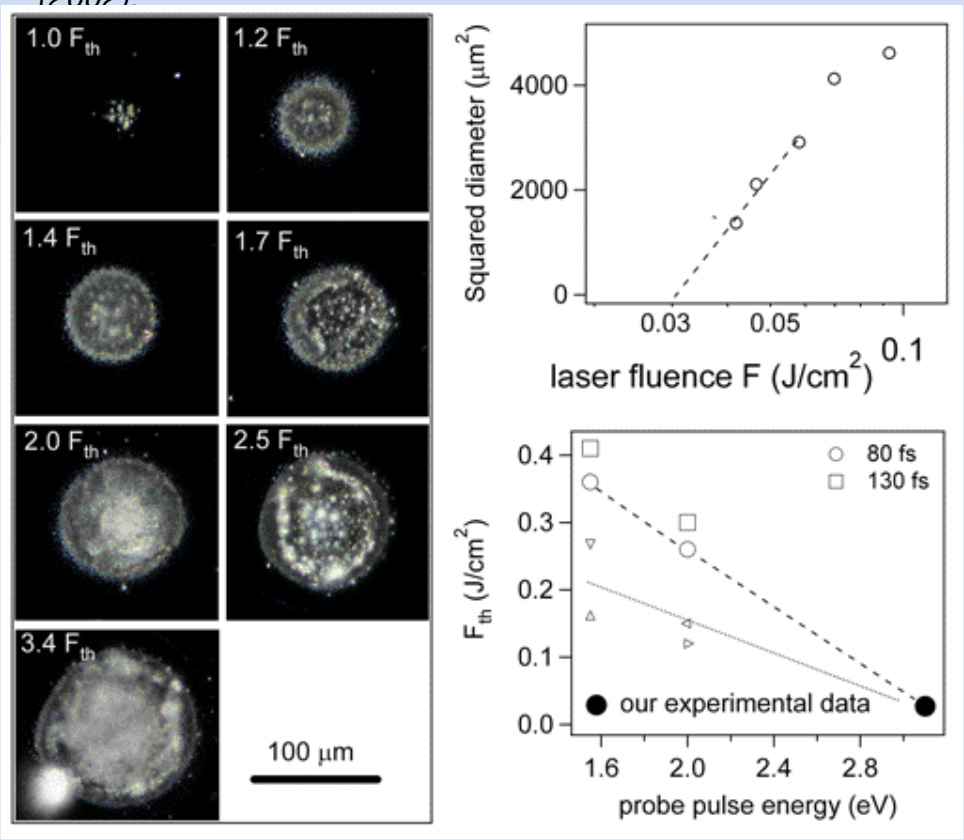

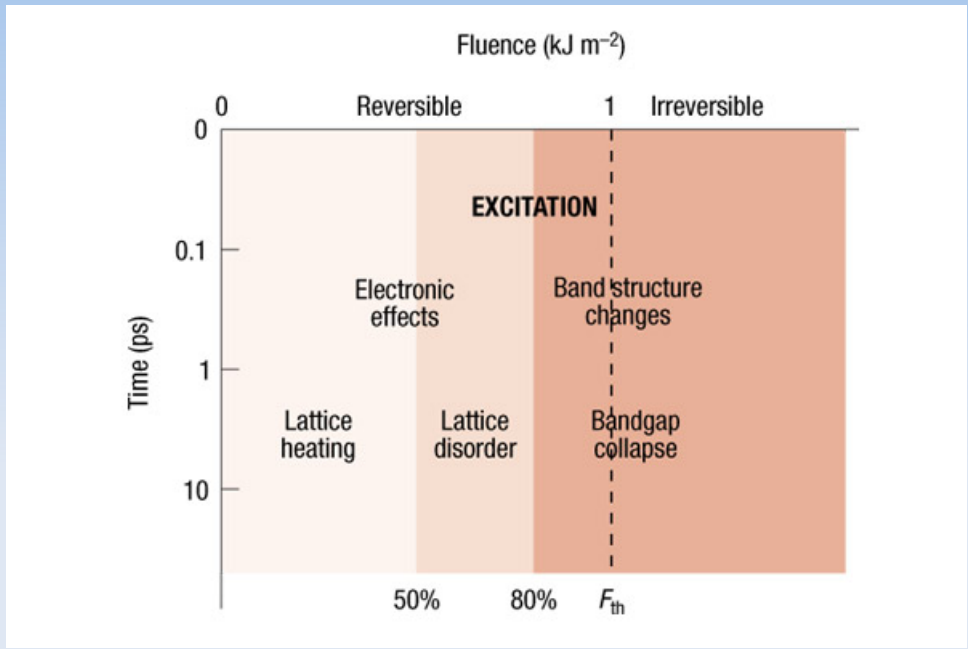

Optical microscope images of the Si(100) surface for different pulse intensity. The damage threshold (F_{Th}) is in line with previous estimates.

Pump energy below the damage threshold

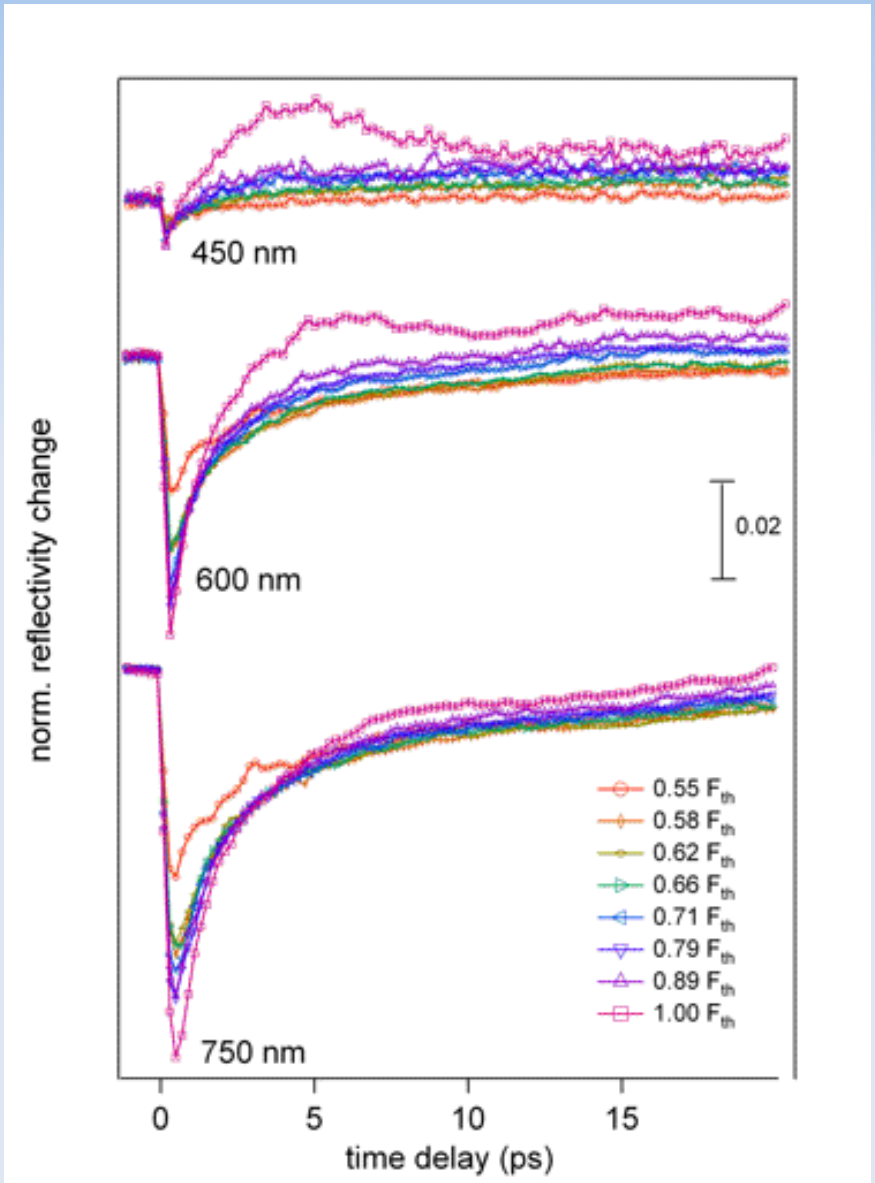

- Ultrafast changes in Si(100) reflectivity strongly depend on the (probe) wavelength.
- Strong negative variations increasing with fluence from 1% to 10% (long wavelengths) within 1 ps, gradual recovery at times ~500 ps.

- The reflectivity change tends to be positive (after 1ps at 400 nm, above 20 ps for longer wavelength).

Pump energy below the damage threshold

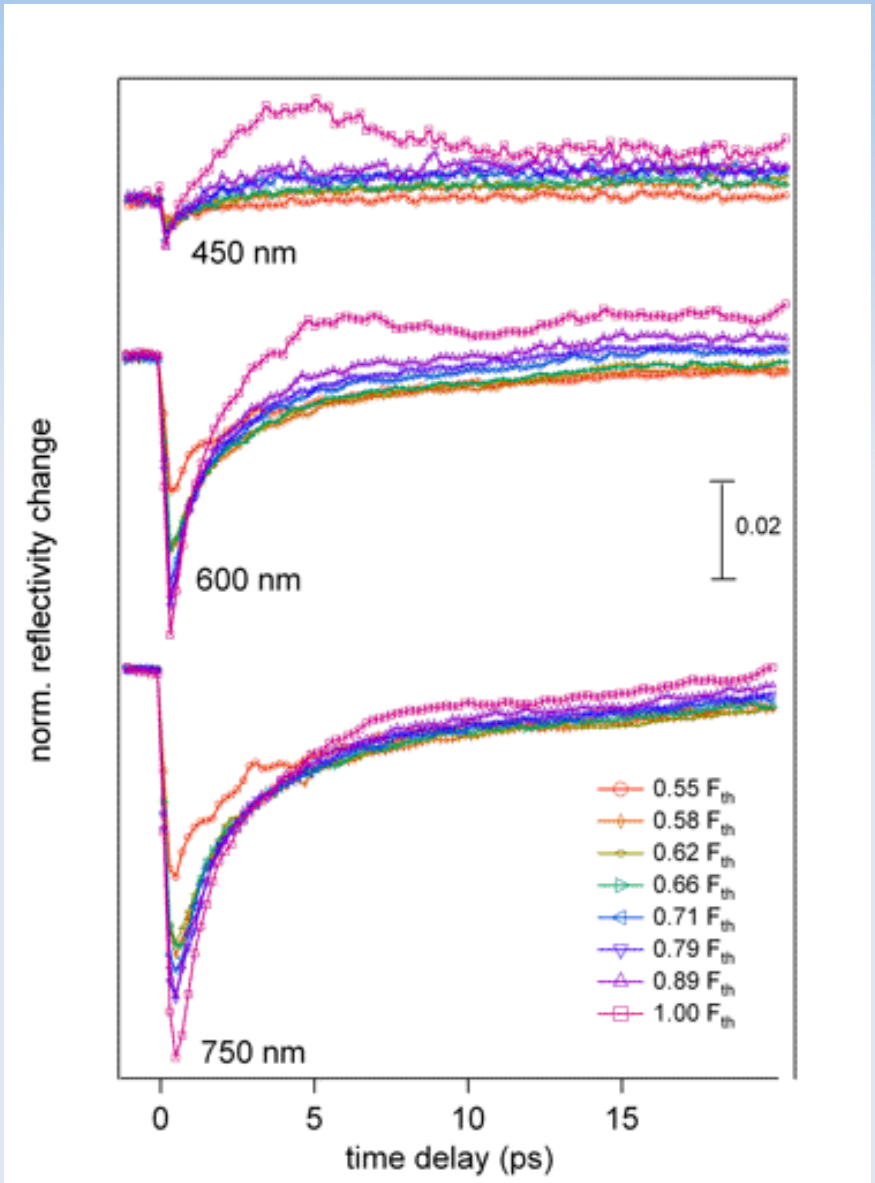

- Ultrafast changes in Si(100) reflectivity strongly depend on the (probe) wavelength.
- Strong negative variations increasing with fluence from 1% to 10% (long wavelengths) within 1 ps, gradual recovery at times ~500 ps.

- The reflectivity change tends to be positive (after 1ps at 400 nm, above 20 ps for longer wavelength).

Summary of Si(100) optical ultrafast data 0.55-1.00 Th
-below damage threshold-

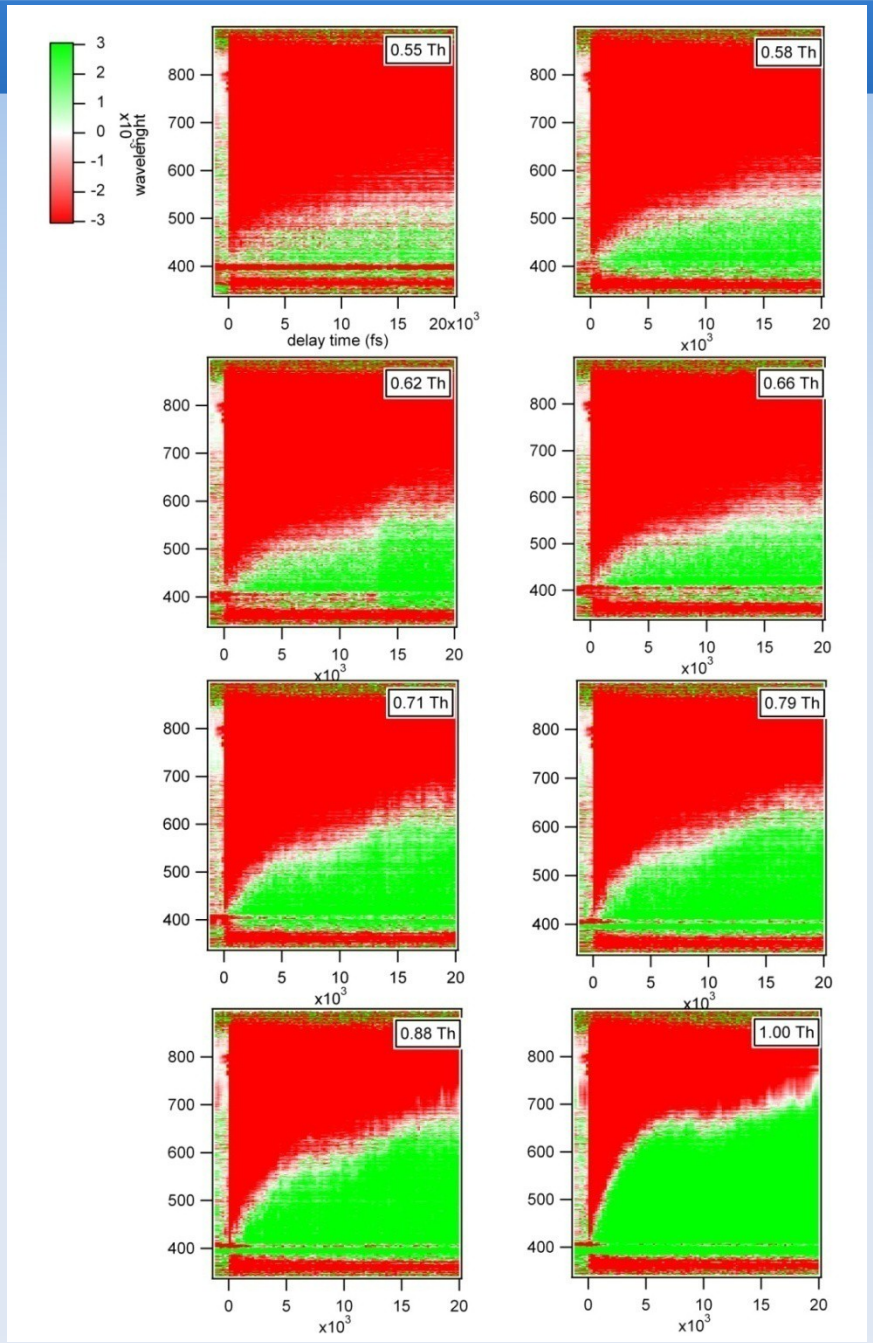

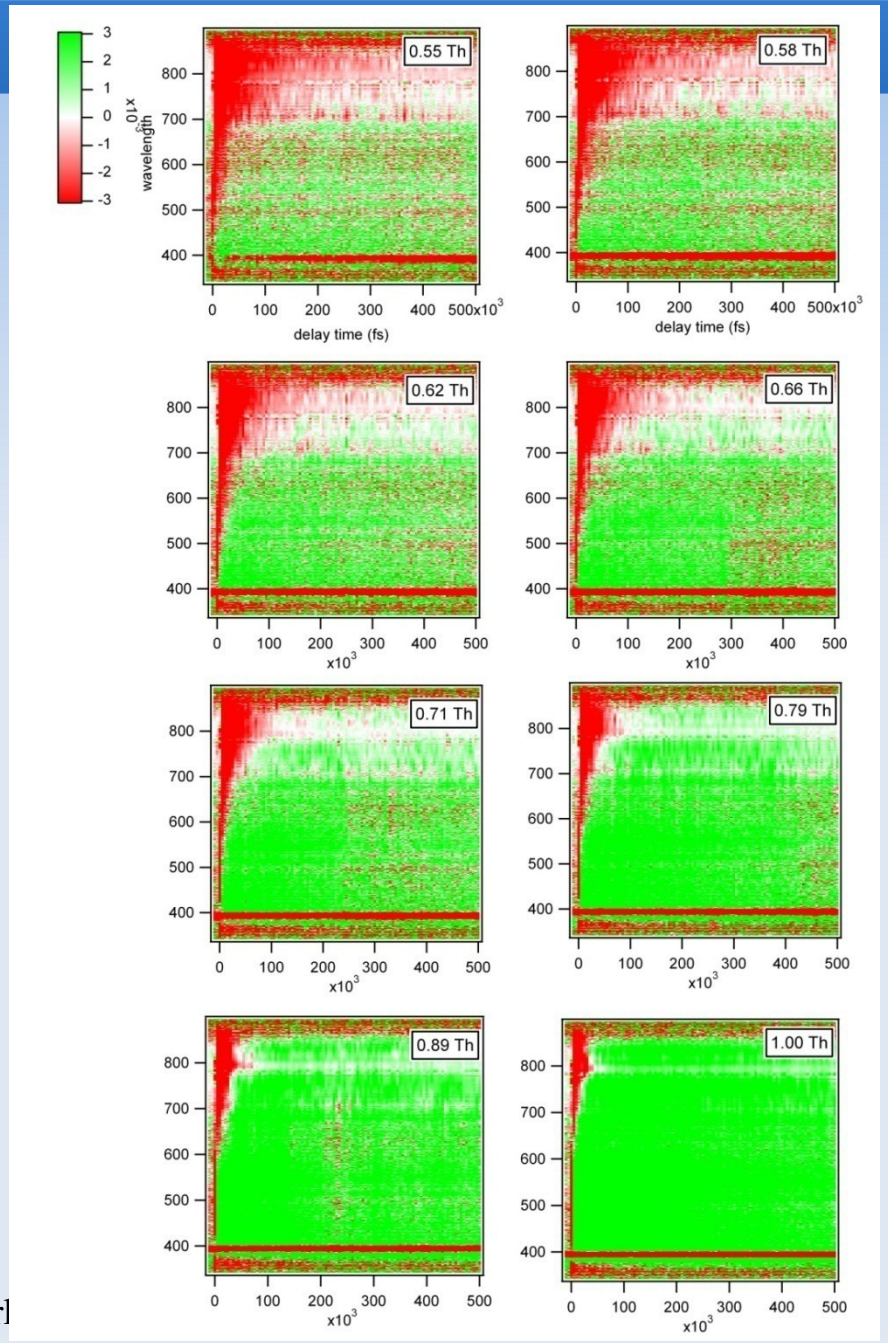

Trend for ultrafast reflectivity

Changes in reflectivity can be calculated modelling the dielectric function (refraction index n).
The change depends mainly on the (time-dependent) number density N(t) of excited electrocns and on the electron temperature Te.
The number density N(t) at short times is well described by an exponential decay of the initial excitation density N_{in} (relaxation time t~10 ps). The excess energy of about 1.8 eV (hv-Eg) correspond to initial temperatures up to 20000 K for the electrons. The hot carriers thermalize with the lattice with a time constant $\tau_{el\text{-}ph}$ ~260 fs (PRB vol. 66, 165217).

For our temporal resolution (100 fs) we expect to see 3 contributions:

1) free-carrier (FC) contribution (Drude-like)
– *negative*
2) state-filling (SF) associated with the absence of electrons in the valence band, lowering the absorption coefficient
- *negative*
3) lattice heating effects as a consequence of electron thermalization (variation of the refraction index with temperature)
-*positive*

PHYSICAL REVIEW B **66**, 165217 (2002)

Femtosecond pump-probe reflectivity study of silicon carrier dynamics

A. J. Sabbah and D. M. Riffe
Physics Department, Utah State University, Logan, Utah 84322-4415

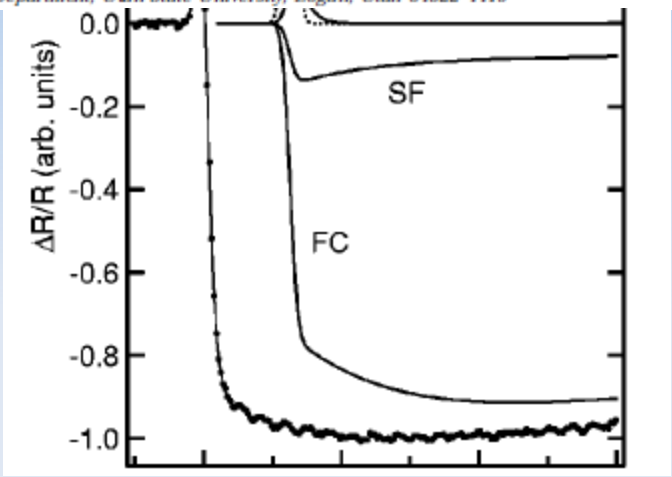

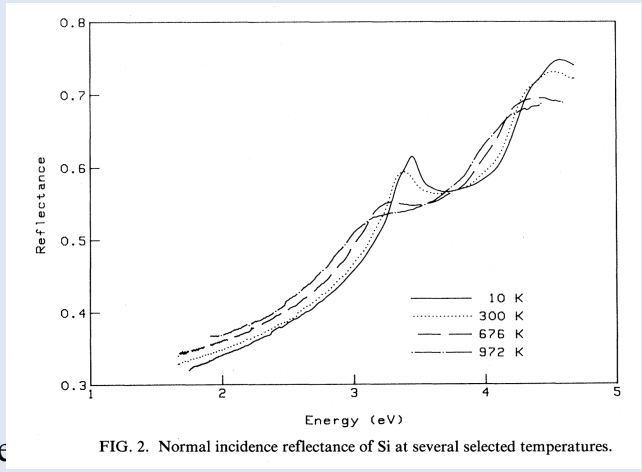

FIG. 2. Normal incidence reflectance of Si at several selected temperatures.